Journal of Medicinal Chemistry

Article

Molecular Design and Synthesis of Ivermectin Hybrids Targeting Hepatic and Erythrocytic Stages of Plasmodium Parasites

Lovepreet Singh, Diana Fontinha, Denise Francisco, Antonio M Mendes, Miguel Prudêncio, and Kamaljit Singh

J. Med. Chem., **Just Accepted Manuscript** • DOI: 10.1021/acs.jmedchem.0c00033 • Publication Date (Web): 03 Feb 2020

is published by the American Chemical Society. 1155 Sixteenth Street N.W., Washington, DC 20036

Molecular Design and Synthesis of Ivermectin Hybrids Targeting Hepatic and Erythrocytic Stages of *Plasmodium* Parasites

*Lovepreet Singh,[1] Diana Fontinha,[2] Denise Francisco,[2] Antonio M. Mendes,[2] Miguel Prudêncio[2] and Kamaljit Singh[1,]**

[1]Department of Chemistry, Guru Nanak Dev University, Amritsar – 143 005, India

[2]Instituto de Medicina Molecular, Faculdade de Medicina da Universidade de Lisboa, Av. Prof. Egas Moniz, 1649-028 Lisboa, Portugal

KEYWORDS: Ivermectin, Hybrids, Antiplasmidial, Liver-Stage, Blood-Stage, Glutamate-Gated Chloride Channels

ABSTRACT

Ivermectin is a powerful endectocide, which reduces the incidence of vector-borne diseases. Besides its strong insecticidal effect on mosquito vectors of the disease, ivermectin inhibits *Plasmodium falciparum* sporogonic and blood stage development, as well as impairs *P. berghei* development inside hepatocytes, both *in vitro* and *in vivo*. Herein, we present the first report on structural modification of ivermectin to produce dual-action molecular hybrids with good

structure-dependent *in vitro* activity against both the hepatic and erythrocytic stages of *P. berghei* and *P. falciparum* infection, suggesting inclusion of ivermectin antimalarial hybrids in malaria control strategies. The most active hybrid displayed over 3-fold and 10-fold higher *in vitro* activity than ivermectin against hepatic and blood stage infections, respectively. Although an overwhelming insecticidal effect against *Anopheles stephensi* mosquitoes in laboratory conditions was not noticed, *in silico* docking analysis supports allosteric binding to glutamate-gated chloride channels similar to ivermectin.

INTRODUCTION

In pursuance of the efforts towards elimination of malaria from endemic regions, the last decade has witnessed reasonable success in controlling malaria-related morbidity and mortality. However, progress appears to be slow and, according to the *World Malaria Report 2019,*[1] 228 million cases and 405 000 deaths were attributed to malaria in 2018, compared to 435 000 estimated malaria-related deaths in 2017.[2] These statistics raise serious concerns regarding the success of the global malaria eradication efforts, and constitute a strong basis for adopting integrated approaches involving vector control, as well as the development of new, more efficacious agents targeting *Plasmodium* parasites, the causative agents of the disease.[3]

Plasmodium infection starts when an infected female *Anopheles* mosquito bites a human host to draw a blood meal. During this process, sporozoites enter the blood vessels and are transported to the host's liver, infecting hepatocytes and initiating an asymptomatic hepatic stage of development, during which they multiply asexually into thousands of merozoites.[4] Merozoites are eventually released into the blood, where they cyclically invade and multiply inside erythrocytes, leading to the onset of the clinical symptoms of malaria.[5,6] In *P. vivax* and *P. ovale*, the sporozoites (spz) sometimes differentiate into uninucleate forms called hypnozoites, which

can remain dormant for upto years in hepatocytes only to reactivate and produce active merozoites causing late relapses of malaria, thus complicating treatment strategies.[7] Further, a proportion of the merozoites undergoes sexual development to form male and female gametocytes, which can be taken up by a mosquito during a subsequent blood meal. In the mosquito midgut, parasites undergo a sexual phase of replication that culminates in the formation of infective sporozoites, ready to initiate a new mammalian infection.[8]

Drugs targeting the liver stage of *Plasmodium* infection are highly desirable, not only because of their prophylactic potential, but also because they are potentially able to eliminate hypnozoites. Currently available treatments targeting hypnozoites are the 8-aminoquinoline-based primaquine and tafenoquine.[9] Tafenoquine is considered as advancement over primaquine, since it is administered as a single dose regimen, in contrast to 14-day therapeutic regimen of primaquine. However, both these drugs are associated with intra-vascular haemolysis in glucose-6-phosphate dehydrogenase (G6PD)-deficient patients[10] and neither is recommended in pregnancy and lactation.[11]

Among several reasons of the declining success of malaria eradication is the widespread resistance of *Anopheles* mosquito vectors against insecticides,[12] as well as the emergence of drug-resistant strains of *P. falciparum*, the deadliest human-infective malaria parasite species.[13] Thus, new drugs need to be developed as a viable alternative to counter the diminishing efficacy of quinoline[14] and artemisinin-based[15] interventions, the emerging resistance against these therapies,[16] and limitations of primaquine and related drugs. Targeting *Plasmodium* transmission is also seen as a critical step towards meeting the demanding goals of an eradication agenda.[17]

Ivermectin (Scheme 1), a member of the avermectin family, is a macrocyclic lactone consisting of a mixture of 22,23-dihydroavermectin B1a **1** and 22,23-dihydroavermectin B1b **2**

(80:20).[18] It is a fermentation product of *Streptomyces avermitilis* and a potent endectocide.[19] Ivermectin has been employed against neglected filarial diseases, such as lymphatic filariasis and onchocerciasis,[20] as well as for the treatment of strongyloidiasis,[21] scabies,[22] pediculosis,[23] gnathostomiasis[24] and myiasis.[25] The ivermectin aglycon **3** has structural analogy to milbemycins:[26] milbemycin ∝ 1**4a**, which is a well-known anthelmintic agent that also displays an insecticidal effect and nemadectin **4b**, which is an antibiotic with a broad-spectrum endectocidal and nematocidal activity. Owing to its ability to disrupt parasite transmission by the vector[27,28,29] and inhibit sporogony of *P. falciparum* in *An. gambiae* at sub-lethal concentrations, ivermectin acts as a malaria transmission control drug.[30] The development of a slow-release formulation for mass drug administration (MDA) of ivermectin to control malaria transmission is currently underway.[31]

Ivermectin was recently shown to inhibit the blood stages of *P. berghei* (*in vivo*)[32] and *P. falciparum* (*in vitro*), as well as *Plasmodium* hepatic infection both *in vitro* and *in vivo*.[33] Ivermectin reduces the infection of human hepatoma cells *in vitro* with an effectiveness comparable to that of primaquine (IC_{50} = 2.1 μM and 2.4 μM, respectively).[33] Thus, combined effects of ivermectin against *Plasmodium* sporogonic, hepatic and erythrocytic stages, highlight its potential as a multistage malaria intervention strategy. However, a detailed understanding of the structural features that account for its potent antiparasitic effects is still lacking. We previously reported on the design of pyrimidine-aminoquinoline hybrids, which demonstrated structure-based potent antiplasmodial activity[34-40] against the blood stages of chloroquine resistant (CQ^R: 3D7, Dd2) and sensitive (CQ^S: NF54, D10) *P. falciparum* strains at nM concentration.[36] Primaquine-pyrimidine hybrids with dual mode of action, targeting both the liver and the blood stages of *Plasmodium* infection, have also been reported.[40]

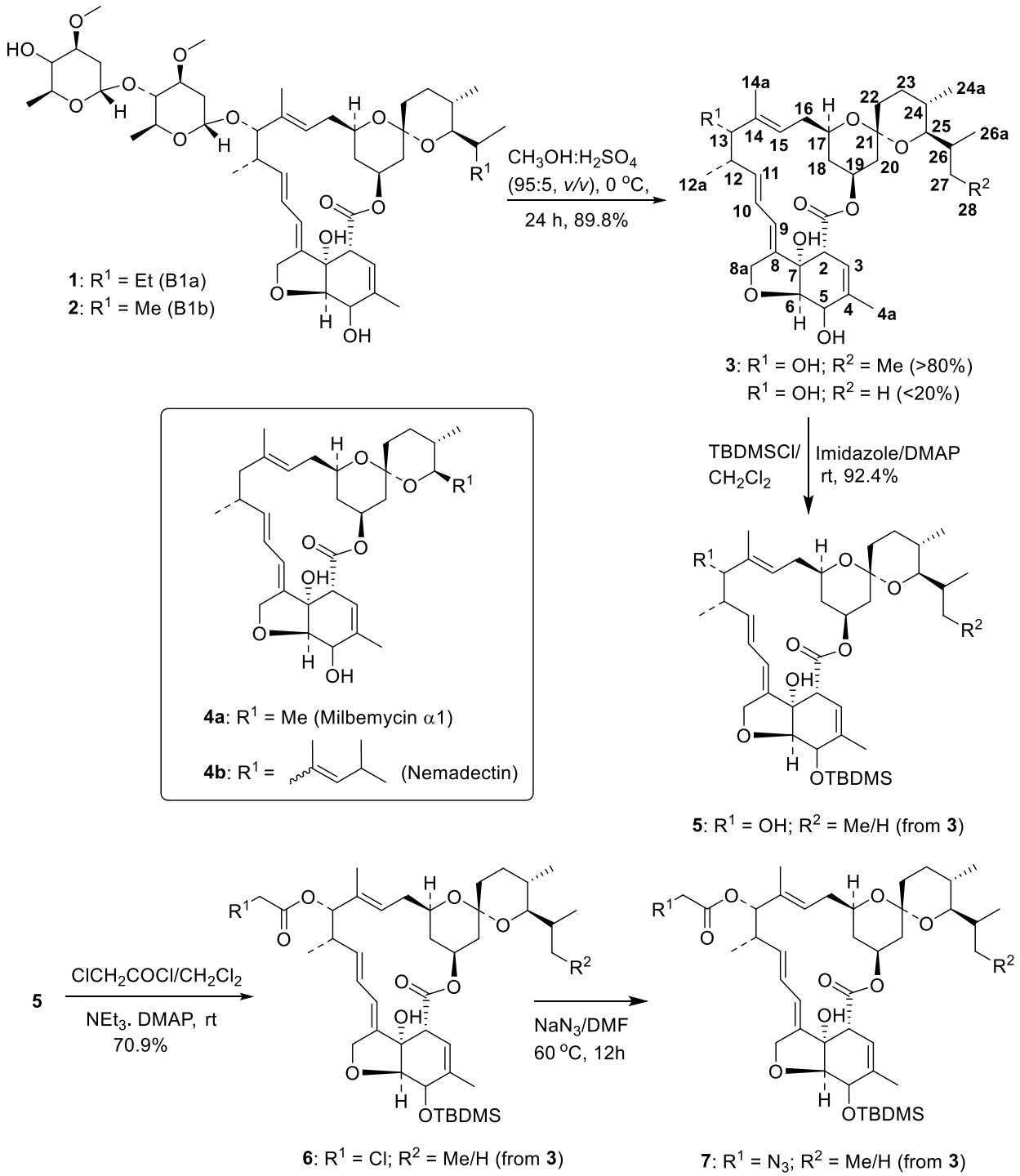

Scheme 1. Chemical structure of ivermectin (**1**/**2**), aglycon **3**, milbemycins **4a** (milbemycin ∝1) and **4b** (nemadectin), numbering scheme of **3** and synthesis of ivermectin azide **7**.

In our continued pursuit for new antiplasmodial hybrids,[41,42] we now report the synthesis and characterization of the antiplasmodial and insecticidal activity of a new class of ivermectin-based hybrid molecules. Several members of this class display enhanced activity against *Plasmodium* relative to the parent ivermectin compound, with the most active member of this series showing at least 3- and 10-fold higher activity than ivermectin against hepatic and blood stage *in vitro* infections, respectively. It has been demonstrated that the invertebrate glutamate-gated chloride channel (GluCl) of the Cys-loop family constitutes a primary target of ivermectin in *A. gambiae*[43] and the X-ray structure of a eukaryotic GluCl co-crystallized with ivermectin has been determined. Ivermectin binds to the exposed sites on the transmembrane domains of the receptor[44] and is visualized as a partial allosteric agonist. Thus, we have investigated *in silico* the binding of the most potent member of this series of ivermectin hybrids to GluCl, showing that it also binds on the transmembrane domain of GluCl and several key binding interactions with specific amino acid residues have been identified. However, the lead compound did not display good insecticidal activity against *An. stephensi* mosquitoes, suggesting that further structure tuning of these hybrids may be critical for preserving their insecticidal activity of ivermectin.

RESULTS AND DISCUSSION

Chemistry: Ivermectin was converted into its aglycon **3** by treatment with 5% H_2SO_4 in methanol, as previously described.[45] Since the –OH group at the C-5 position (Scheme 1) is essential for the effectiveness of ivermectin,[46] it was protected[45] by using *tert*-butyl dimethylsilyl chloride (TBDMS-Cl) to obtain intermediate **5** with 92.4% yield (Scheme 1). Chloroacetylation of **5** using chloroacetyl chloride, triethyl amine in the presence of 4-dimethylaminopyridine (DMAP) furnished intermediate **6** in 70.9% yield. Reaction of **6** with sodium azide gave the

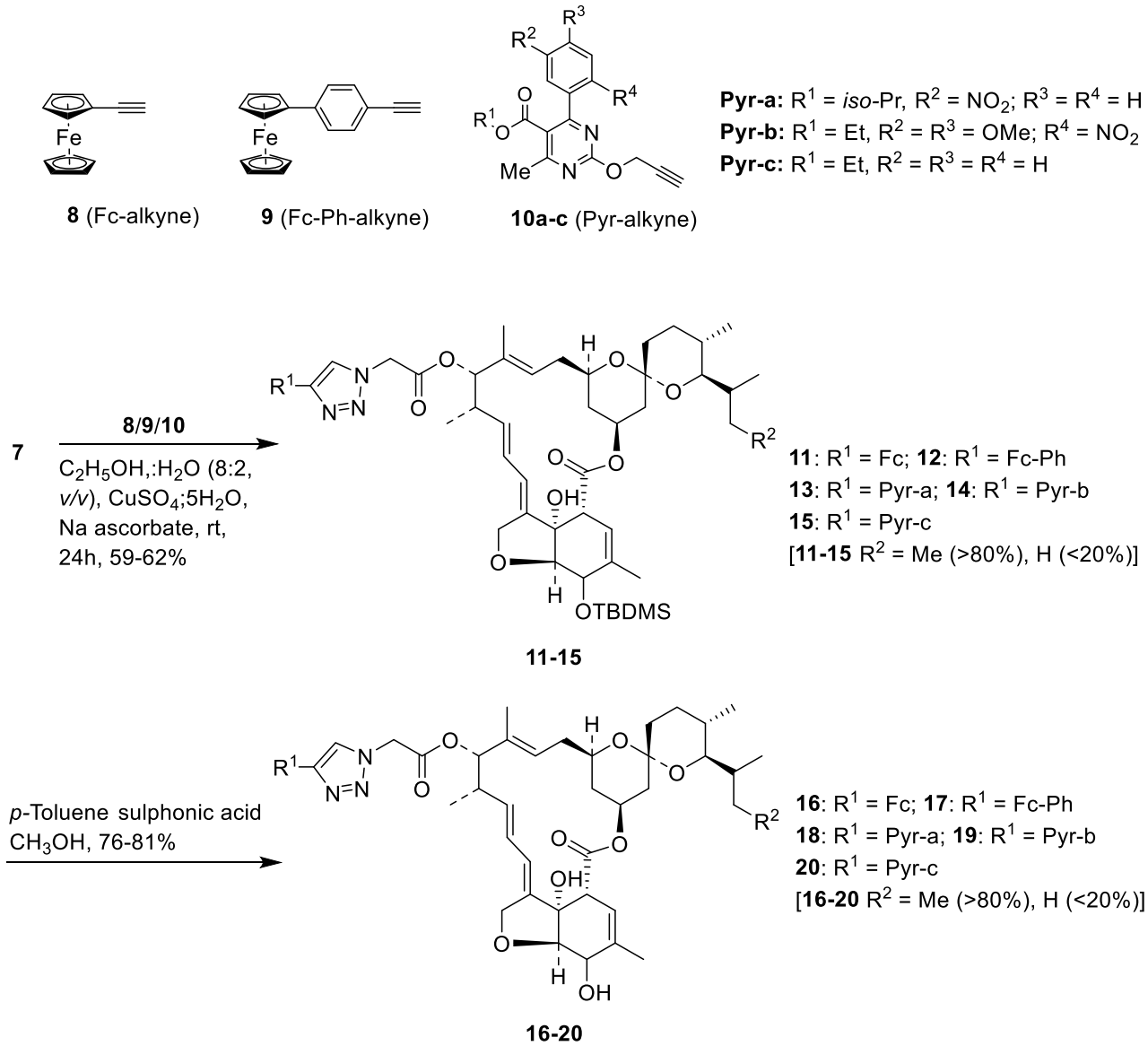

Scheme 2. Structures of alkyne intermediates **8-10** and synthesis of ivermectin hybrids **16-20**.

corresponding azide **7**, which served as a common intermediate for conducting Cu^{+}-mediated azide-alkyne Huisgen 1,3-dipolar cycloaddition reaction (click reaction)[47] with different alkynes (Scheme 2). Azide **7** was not isolated as it showed significant degradation during chromatographic purification and therefore was used in subsequent transformations as such. Alkynes **8-10** were obtained by using reported methods[38] and their reaction with **7** furnished

triazole derivatives **11-15** (Scheme 2), respectively, in 59-62% yield. Triazole derivatives **11-15** were deprotected using *p*-toluene sulphonic acid in methanol to obtain final ivermectin hybrids **16-20**, respectively (Scheme 2) in 76-81% yield. Compound **15** was not very stable and was thus transformed directly to the corresponding **20**. The choice of using a triazole linker to link the pharmacophores was guided by the established therapeutic potential of triazoles such as antitubercular,[48] anticancer[49] and antimalarial[50] agents, as exemplified by drugs such as fluconazole and alprazolam.[51] Similarly, the ferrocene-based hybrid partners were chosen considering the antimalarial efficacy of ferroquine, which is also a derivative of ferrocene.[52] The dihydropyrimidine hybrid partner has been widely used by us[34-40] and others[53] in designing antimalarial agents, which have shown significant activity against both CQ^S as well as CQ^R strains of *P. falciparum*. Further, pyrimidine-based drugs such as cycloguanil and pyrimethamine are also potent antimalarials, which act by inhibiting dihydrofolate reductase.[54,55]

All compounds were unambiguously characterized by spectroscopic techniques and the spectral data is presented in the experimental section and in Supporting Information (Supporting Information, Figures S1-S45, S54-S59). ^{1}H NMR spectral assignments of all intermediates and compounds were performed on the basis of their coupling connectivity as seen in the ^{1}H-^{1}H homonuclear COSY spectrum and confirmed by HRMS and/or microanalytical data. As an example, the 2D COSY spectrum of **17** is shown in Figure 1. The most downfield signals corresponded to the aromatic protons (ArH_1 and ArH_2), adjacent to the triazole and ferrocene units, respectively. The *trans* alkene protons H_{10} and H_{11} could be readily distinguished by their cross-peaks in the COSY spectrum (Figure 1A). Likewise, the *spiro*-tetrahydropyran ring resonances could be identified as depicted in Figure 1B. The H_{15}, H_{17}, H_{25} *etc*. All resonances

embedded among other signals could be assigned on the basis of the coupling network in the COSY spectrum (Figure 1C).

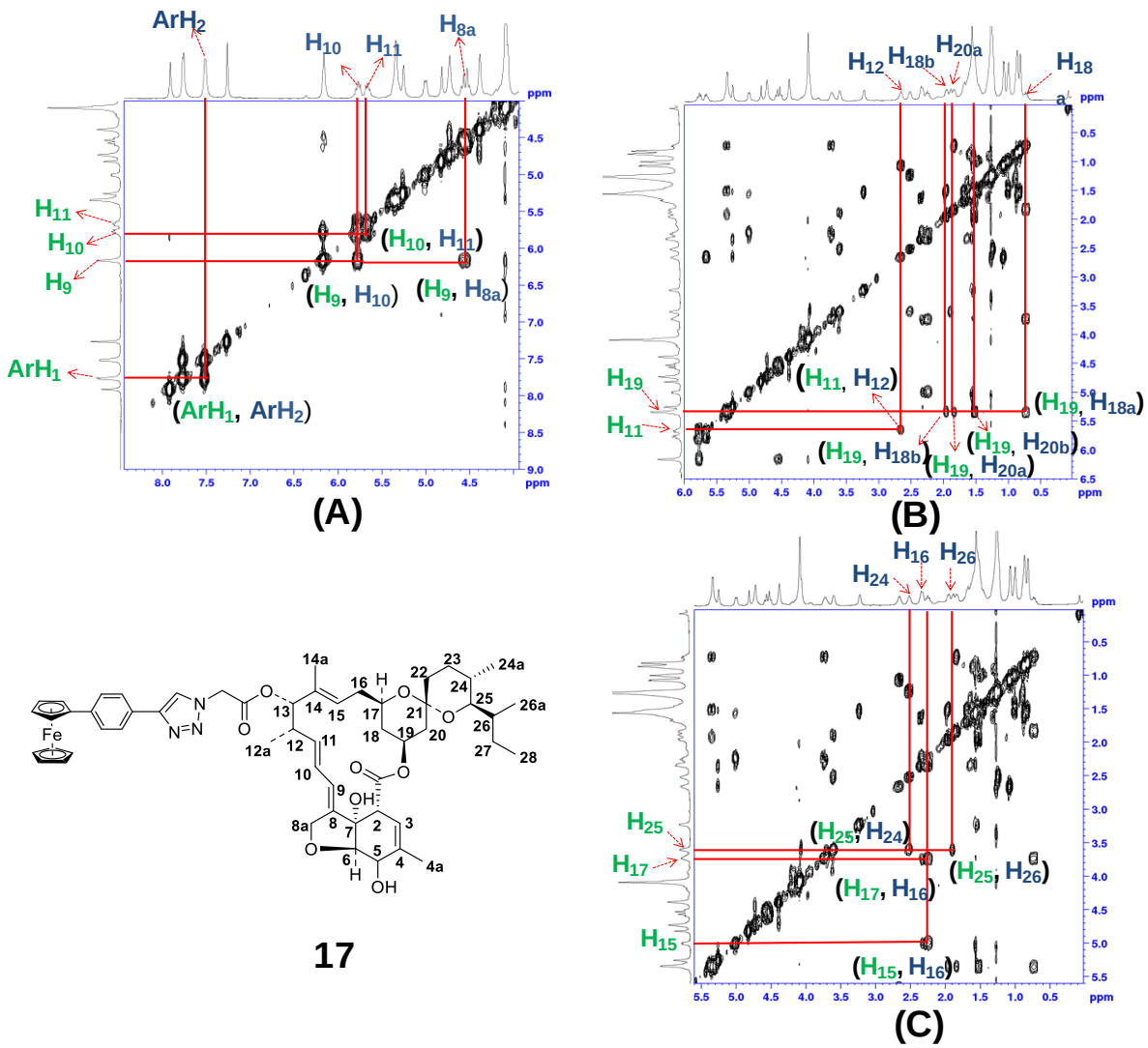

Figure 1. Expanded-scale contour plots of a 500 MHz 2D COSY spectrum of different resonances of hybrid **17** in $CDCl_3$ at 300 K. The coupling networks for the key protons are highlighted.

Chromatographic purification of ivermectin derivatives rendered all compounds pure enough to yield correct spectroscopic data consistent with the composition corresponding to B1a and B1b (Scheme 1) in the precursor ivermectin or the agylcon **3**.

Biology

Antiplasmodial Activity and Structure−Activity Relationships (SARs).

In vitro activity against Plasmodium hepatic and erythrocytic infection and SAR

Ivermectin hybrids **11-13**, **16-20** were initially screened for their *in vitro* activity against the hepatic stage of *P. berghei* infection at 1 and 10 μM (Supporting Information, Figure S46). Hybrids **11**, **12** and **13** did not impact *P. berghei* infection at the concentrations tested. Compounds **16**, **18-20** and the ivermectin aglycon **3** (Scheme 1) presented measurable activity and were consequently selected for IC_{50} determination (Figure 2). Importantly, none of the compounds was toxic to the hepatic cell line at the tested concentrations, as assessed by the measurement of cell confluency (Figure 2). Compound **3**, the ivermectin aglycon, presented the lowest activity among the compounds selected for IC_{50} determination, with an estimated IC_{50} of 4.557 ± 1.98 μM (Table 1). Compounds **16**, **18**, **19** and **20** were more active against the hepatic stage of *P. berghei* infection than the parental ivermectin. Compound **19** was the most active, with an estimated IC_{50} of 0.503 ± 0.002 μM and was 3-fold more active than ivermectin and nearly 9-fold more active than the ivermectin aglycon **3**, corroborating the hypothesis that molecular modification of ivermectin can produce more active compounds. Notably, compound **19** was 2.5-fold more active against the liver stage of infection than the most active member of the pyrimidine-primaquine hybrids (IC_{50} = 1.261 ± 0.310 μM)[40]. The correlation of the hybrid structures with their liver stage antiplasmodial activity allows the identification of structural features responsible for activity. Thus, appending ferrocene (**16**) or a substituted pyrimidine

bearing C-4 aryl (Ar: 3-nitrophenyl **18** and 2-nitro-3,4-dimethoxy phenyl **19** and phenyl **20**) and a C-5 carboxylate ester (*iso*-propyl **18**, ethyl **19**/**20**) moieties, and retaining a free C-5 OH on the macrolide moiety, enhances liver stage activity. Conversely, the corresponding hybrids bearing a bulkier hydrophobic *tert*-butyldimethylsilyl (TBDMS) group at 5-OH group of the macrolide unit proved detrimental to the liver stage antiplasmodial activity, as illustrated (Supporting Information, Figure S46) by hybrids **11**-**13**, bearing a TBDMS group at 5-OH.

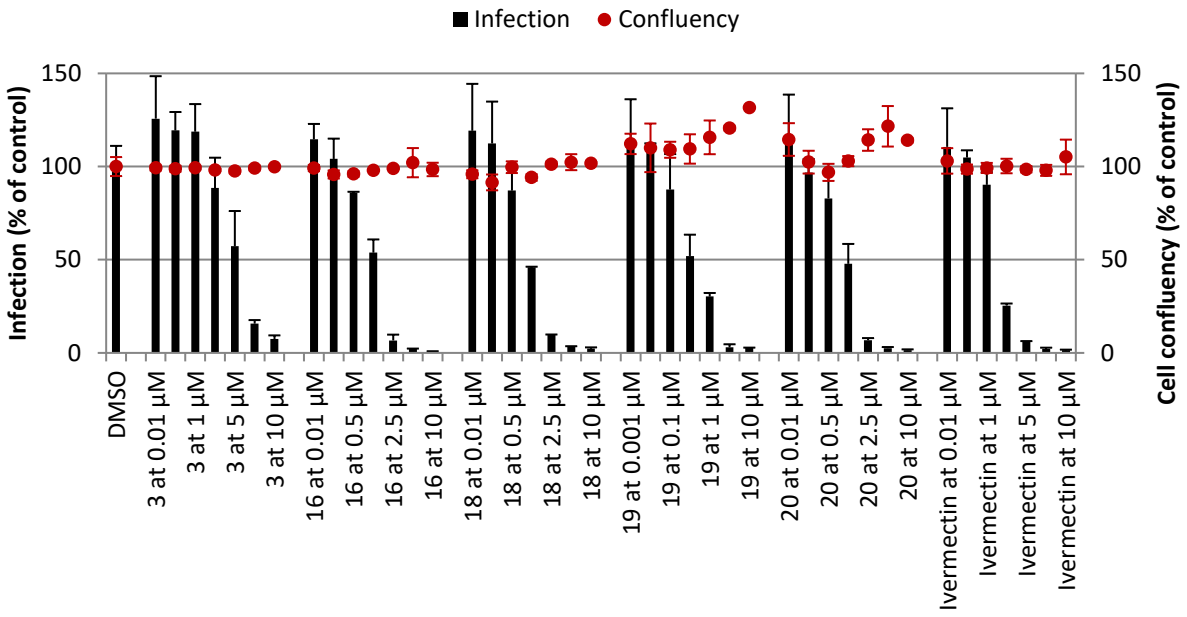

Figure 2. Dose-dependent response of ivermectin-based hybrids (**16**, **18**, **19**, **20**), ivermectin aglycon **3** and ivermectin against the hepatic stage of *P. berghei* infection. Total parasite load (infection scale, bars) and cell viability (cell confluency scale, dots) are shown. Calculated IC_{50} values are presented in Table 1.

Table 1. IC_{50} values of selected compounds against the hepatic stage of *P. berghei* and the erythrocytic stage of *P. falciparum* NF54.

Compound	IC_{50} (µM) *P. berghei*[a]	IC_{50} (nM) *Pf*NF54[b]
16	0.990 ± 0.068	256.7± 46.6
18	0.911 ± 0.076	161.2± 40.9
19	0.503 ± 0.002	50.2± 24.5[c]
20	0.990 ± 0.050	110.5± 64
3	4.557 ± 1.981	na
Ivermectin	1.639 ± 0.189	519.6± 175.4
CQ	-	23.7±10.1
ATQ[d]	0.0007 ± 0.057	-

[a]Results are represented as mean ± SD, n ≥ 2; [b]chloroquine sensitive (CQ^S) strain; [c]the lowest value was 23.7 nM; [d]Atovaquone; na: Not active at the tested concentrations.

Encouraged by the results of the hepatic stage activity, these compounds were also assessed for *in vitro* activity against the CQ^S *Pf*NF54 *P. falciparum* strain, using ivermectin and chloroquine as controls. Whereas the ivermectin aglycon **3** did not shown any significant blood stage antiplasmodial activity at the tested concentrations, the structurally modified hybrids **16**, **18**, **19** and **20** were ~2-, ~3-, ~5- and ~11-fold more active against infection than the ivermectin parent compound, respectively (Table 1). Our results show that these compounds display similar relative antiplasmodial activity profiles during the hepatic and blood stages of infection. Thus, while compounds **16**, **18**, **19** and **20** are consistently more active than both ivermectin and the aglycon **3**, compound **19** emerged as the strongest antiplasmodial compound of the series against

both infection stages (Table 1). These results demonstrate that the structure of ivermectin can effectively be tuned through chemical modification to produce more active antiplasmodial agents.

Insecticidal activity against An. stephensi mosquitoes

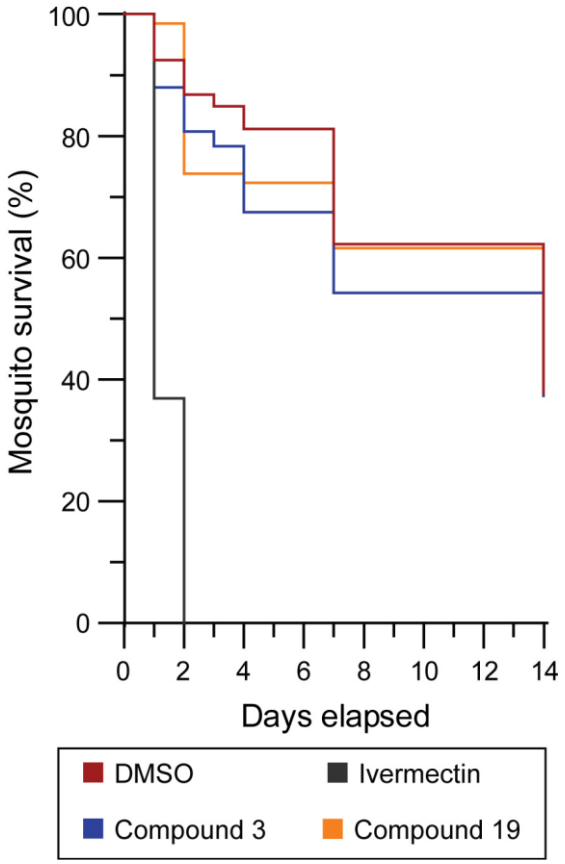

Figure 3. Mosquito survival following administration of **19** and **3**,ivermectin and DMSO in mice.

Since avermectins in general, and ivermectin in particular, have a strong insecticidal effect against *An*. mosquitoes,[27] we examined the insecticidal activity of the most active member of the series, compound **19**, and of ivermectin aglycon **3**, employing ivermectin and DMSO as positive and negative controls, respectively. A single dose 1 mg/kg of each compound was administered

to C57B1/6 mice by oral gavage. Mosquitoes were then allowed to feed on the blood of these mice 24 h after compound administration, and mosquito survival was subsequently monitored for 14 days (Figure 3). Our results show that, unlike ivermectin, neither of **19** or **3** displayed any significant insecticidal activity against *An. Stephensi* mosquitoes. These results are in agreement with the previous observation that macrolide aglycon **3** displays significantly lower insecticidal activity than ivermectin when tested against first-instar *Lucia sericata* blowfly larvae.[56] Thus, although the current design of hybrids, which employs ivermectin aglycon with the sugar residue at C-13 replaced with a hybrid partner (*vide supra*), enhances ivermectin's antiplasmodial effect against both the liver blood stages of *Plasmodium* infection, it also significantly impacts ivermectin's insecticidal activity. The lack of such activity by compound **19** can be, at least in part, attributed to the absence of the sugar unit at C-13 position (Scheme 1) of ivermectin. Another possibility concerns possible differences in the blood levels of each compound following their oral administration, which might differ between compounds. Nonetheless, the insecticidal effect of ivermectin does not appear to be essential for its antiplasmodial activity, as the drug appears to act on different targets in the parasite and in the mosquito. In invertebrates, ivermectin interacts with the GluCl channels in neuromuscular and neuronal tissues[57-59] and may also act on the γ-aminobutyric acid-gated chloride channels.[60,61] However, neither of these molecular targets is present in *P. falciparum*. Conversely, ivermectin has been suggested to inhibit the blood stage development of the parasite by blocking nucleo-cytoplasmic shuttling of *P. falciparum* signal recognition particle components,[32] although this is a matter of some controversy.[62] Furthermore, it has recently been shown that, while ivermectin is inactive against *P. berghei* gametocytes, both ivermectin and other members of the avermectin family strongly inhibit parasite sporogony, independently of their insecticidal effect.[63] Collectively, these results

and the ones presented in the current manuscript support the notion that ivermectin acts independently on the mosquito and on the parasite.

The absence of any sizeable effect of compound **19** on mosquito survival raised the question as to whether it lacked the ability to bind with GluCl, which has been characterized as the primary target of ivermectin in invertebrates, including *A. gambiae* mosquitoes.[43] Thus, we probed (Supporting Information, page 45) the binding of compound **19**, to the pocket of GluCl-Fab (Schrödinger Release 2019-2: Glide, Schrödinger, LLC, New York, NY, 2019).[44] In a manner similar to ivermectin, hybrid compound **19** was also found to bind at transmembrane domains on the subunit interface towards the extracellular side of GluCl-Fab (PDB ID 3RHW) (Figure 4). Compound **19** is immersed deep into the subunit, making several key contacts with specific amino acid residues. For example, the deeply buried C-7 OH of **19** shows a strong hydrogen bonding interaction (1.83 Å) with the Leu218 residue located on the M1 (-) helix, whereas the C-5 OH of **19** forms a hydrogen bond (1.91 Å) with Gln219 on the M2 (-) helix. The C-5 OH of **19** also makes hydrogen bonding (2.65 Å) interaction with Ser260 located on the M2 (+) helix. Further, the oxygen atom of one of the spiro-tetrahydropyran rings makes weak hydrogen bonded (3.47 Å) with Thr285 on the M3 (+) unit. Tracing the binding interactions of the hybrid partner pyrimidine subunit of **19** revealed no binding interaction as it is oriented outside the protein complex and resides at an allosteric site. In analogy to the mode of binding of ivermectin, our results suggest that the docking of hybrid **19** in GluCl-Fab may induce global conformational changes resulting in the modulation of the ion conductive pathway. However, a definitive explanation of this feature remains elusive.

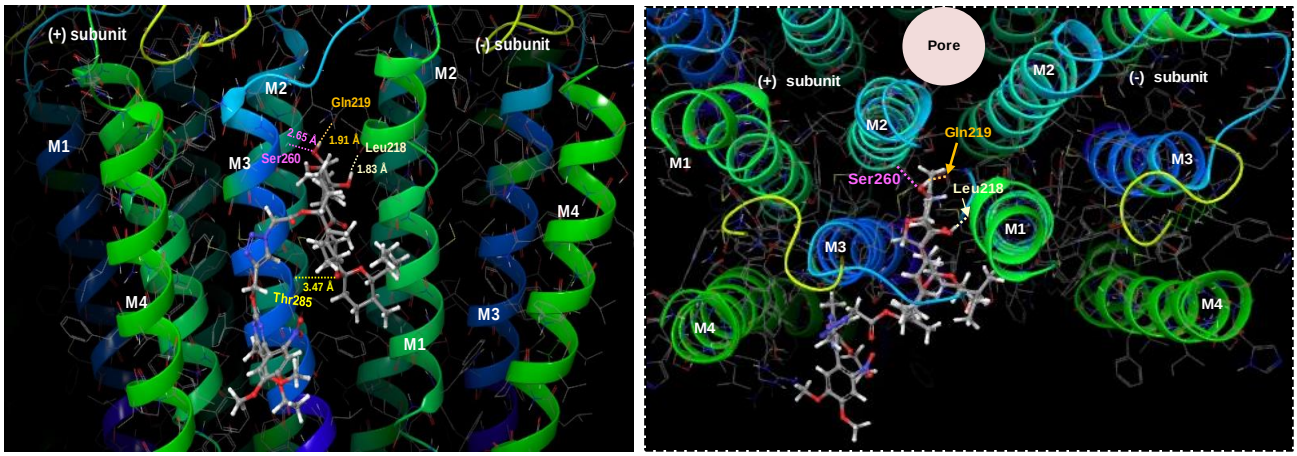

(A) (B)

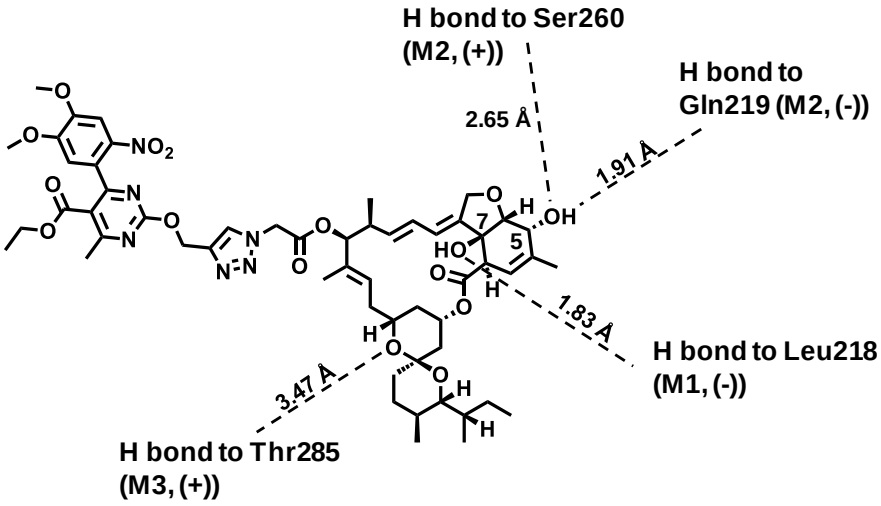

(C)

Figure 4. Binding site and atomic interactions of ivermectin hybrid **19** to the pocket of GluCl-Fab. (A) view from the receptor's periphery, parallel to the membrane, and (B) view from the top, extracellular side, looking down the pore. Pose in (A) is rotated by 90° (along the horizontal plane) and with extracellular domains deleted for a clear view of the GluCl subunit interface, depicting the binding site of ivermectin hybrid. (C) Summary of the key interactions of different atoms with amino acid residues (Glide score: -12.024, Glide energy: -135.48 Kcal/mol).

CONCLUSIONS

The present investigation demonstrates that structure modification of ivermectin constitutes an effective strategy to the design of new leads to counter liver and blood stage *Plasmodium* infection. Our observation that compounds **11-13**, bearing a hydrophobic *tert*-butyl dimethylsilyl (TBDMS) group at the C-5 OH, lack antiplasmodial activity strongly suggests that this position may play a specific role in the overall antiplasmodial activity. Compound **17**, bearing a ferrocenephenyl on the triazole linker at C-13 of the macrolide framework of ivermectin, is bereft of good activity, as seen in the preliminary screening (Figure 41, SI). However, compound **16**, bearing a ferrocene group without a phenyl group, does show enhanced activity (IC_{50} = 0.990±0.068 μM) relative to ivermectin (IC_{50} =1.639±0.189 μM) as well as ivermectin aglycon **3** (IC_{50} =4.557±1.981 μM). The fact that compound **3**, bearing a free OH group at the C-13 position is less active (Table 1) than the hybrid compounds **16**, **18**, **19** and **20** of this series highlights the role of the hybridization partner in enhancing antiplasmodial activity. Out of the three compounds containing a pyrimidine unit as the hybrid partner (**18-20**), compound **18**, bearing an *m*-NO_2 group on the C-4 aryl group in combination with an C-5 *iso*-propyl ester, and compound **20**, bearing an unsubstituted phenyl group at the C-4 position in combination with an C-5 ethyl ester, showed IC_{50} =0.911±0.076 μM and 0.990±0.050 μM, respectively. Thus, the presence of the 2-nitro-4,5-dimethoxyphenyl group at C-4 of the pyrimidine, along with an ethyl ester group at C-5 in **19**, was most favorable, leading to the lowest IC_{50} values for both the liver and the blood stage of infection (0.503±0.002 μM and 50.2±24.5 nM, respectively).

Overall, we found that the advantage gained by appending hybrid partners at C-13 of the macrolide unit in terms of enhancing the antiplasmodial activity of these structurally modified compounds may be somewhat offset by the decrease in their insecticidal activity, which can be

attributed to the lack of the sugar residue at C-13 position. Since the antimalarial potential will be maximized for compounds that simultaneously present antiplasmodial and insecticidal properties, work towards designing and synthesizing such structure modifications is currently in progress.

EXPERIMENTAL SECTION

Chemistry. General. All liquid reagents were dried/purified following recommended drying agents and/or distilled over 4 Å molecular sieves. CH_3CN was dried by refluxing over P_2O_5. DMF was dried overnight by storing over 4 Å molecular sieves. DCM was dried over fused calcium chloride. Chloroacetyl chloride, propargyl alcohol, *tert*-butyldimethylsilyl chloride (TBDMS-Cl) and 4-dimethylaminopyridine (DMAP) were bought from Spectrochem India. Imidazole was bought from Sigma Aldrich. Triethylamine, sodium-(L)-ascorbate and $CuSO_4{\cdot}5H_2O$ were bought from LobaChemie. K_2CO_3 was dried overnight in furnace. ^{1}H NMR and ^{13}C NMR spectra were recorded on Bruker BiospinAvance III HD at 500 MHz, JEOL-FT NMR-AL at 400 MHz and JEOL- FT NMR-AL at 300 MHz with TMS as internal standard using $CDCl_3$ as deuterated solvent. Data are reported as follows: chemical shift in δ (ppm), integration, multiplicity (s = singlet, d = doublet, t = triplet, m = multiplet), coupling constant J (Hz). High Resolution Mass spectra (HRMS) were recorded on a Bruker LC-MS MICROTOF II spectrometer and Waters Synapt G2-Si Q ToF Mass Spectrometer. IR spectra were recorded on Agilent Technologies Cary 630 FTIR spectrometer and Perkin-Elmer FTIR-C92035 Fourier transform spectrometer in the range 400−4000 cm^{-1} using KBr pellets. While the purity of **8** and **9** was ascertained from the microanalytical data, for all other compounds satisfactory HRMS data is provided. Preparative TLC was performed on glass plates using silica gel GF_{254} for TLC bought from Spectrochem India. HPLC was performed in Reverse Phase mode using

Agilent 1260 Infinity series HPLC (Agilent Technologies, USA) equipped with Quaternary Pump VL (G1311C) and degasser, 1260 ALS auto sampler (G1329B) and 1260 DAD VL detector (G1315D). Column used was ZORBAX Eclipse C18 column (4 x 100 mm) (Agilent Technologies, USA). Mobile phase was comprised of a mixture of acetonitrile-methanol-water (49.2:32.8:18 *v/v/v*) and the flow rate was set to 1.0 mL/min. All the solvents used were of HPLC grade. Preparative thin layer chromatography on the compounds, evaluated for biological activity yielded purity of **16**, **18-20** upto 95% as revealed by HPLC analysis (Supporting Information, Figures S48-S53). Thus, the samples of the compounds **16**, **18-20** analyzed for the antiplasmodial and mosquitocidal activity (*vide infra*) are expected to contain the minor component (corresponding to B1b).

General procedure for the synthesis of (3). Ivermectin (5.57 mmol, 5.0 g) was added to methanolic sulphuric acid (50 ml, 95:5, *v/v*). The reaction mixture was stirred at 0 °C for 24 h. Dichloromethane (DCM) (150 ml) was added and the solution was neutralized with aqueous sodium bicarbonate solution (3×20 ml, 5%, *w/v*) followed by washing with water. The organic extract was dried over anhydrous sodium sulfate and solvent was removed under reduced pressure. A yellow colored crude product was isolated which was subsequently purified by chromatography over silica gel (60-120 mesh) using hexane/ethyl acetate (75:25, *v/v*) as the eluent to obtain pure **3** (3 g, 89.8%) as a white solid. IR: ν_{max} 3451.5, 2929.7, 1714.6, 1453.7, 1371.7, 1170.4, 984.0, 492.0 cm^{-1}. ^1H NMR (400 MHz, $CDCl_3$, 25 °C): δ (ppm) 5.67-5.84 (m, 3H, H_9, H_{10}, H_{11}), 5.41 (br, 1H, H_3), 5.27-5.34 (m, 2H, H_{15}, H_{19}), 4.63-4.72 (m, 2H, 2 x H_{8a}), 4.29 (d, 1H, H_5), 4.07 (s, 1H, C_7-OH, D_2O exchangeable), 4.01 (br, 1H, H_{13}), 3.96 (d, 1H, *J = 4 Hz*, H_6), 3.64-3.71 (m, 1H, H_{17}), 3.24-3.26 (m, 1H, H_2), 3.17-3.20 (m, 1H, H_{25}), 2.48-2.54 (m,

1H, H_{12}), 2.26-2.26-2.34 (m, 3H, 2 x H_{16}, H_{26}), 1.95-2.0 (m, 1H, H_{18a}), 1.86 (s, 3H, 3 x H_{4a}), 1.72-1.76 (m, 1H, H_{20a}), 1.30-1.66 (m, 11H, 3 x H_{14a}, H_{20b}, 2 x H_{22}, 2 x H_{23}, 2 x H_{27}, C_{13}-OH, D_2O exchangeable), 1.17 (d, 3H, J = 8 Hz, 3 x H_{12a}), 0.95 (t, 3H, J = 4 Hz, H_{28a}), 0.78-0.83 (m, 7H, H_{18b}, 3 x H_{26a}, 3 x H_{24a}). ^{13}C NMR (125 MHz, $CDCl_3$, 25 °C): δ (ppm) 173.52, 139.75, 138.63, 137.73, 137.04, 124.76, 120.43, 118.18, 117.19, 97.46, 80.25, 79.19, 77.65, 77.23, 68.57, 68.48, 67.73, 67.26, 46.71, 41.35, 40.07, 36.76, 35.81, 35.53, 34.23, 31.27, 28.07, 27.50, 19.93, 19.17, 17.46, 14.46, 14.61, 12.54, 11.77. HRMS: *m/z* $[M+Na]^+$ for $C_{34}H_{50}O_8$, calculated 609.3398; observed 609.3375. t_R(245 nm) = 4.41 min.

Synthesis of (5). To a solution of **3** (1.0 g, 1.7 mmol) in dry DCM (10 ml), DMAP (0.001 g, 0.01 mmol), imidazole (0.578 g, 8.5 mmol) and TBDMS-Cl (0.51 g, 3.4 mmol) were added. The resulting solution was stirred at room temperature for 4 h. Reaction mixture was poured into water and extracted with DCM (3×20 ml). The organic extract was washed with saturated aqueous sodium chloride solution (2×20 ml), dried over anhydrous sodium sulfate. Solvent was removed under reduced pressure and the yellow residue was purified by column chromatography over silica gel (60-120 mesh) using hexane/ethyl acetate (90:10, *v/v*) as the eluent to isolate **5** (1.10 g, 92.4 %) as a white foamy solid. IR: ν_{max} 3473.9, 2929.7, 2862.6, 1714.6, 1461.1, 1371.7, 1170.4, 1080.9, 991.5, 492.0 cm^{-1}. ^1H NMR (400 MHz, $CDCl_3$, 25 °C): δ (ppm) 5.65-5.80 (m, 3H, H_9, H_{10}, H_{11}), 5.22-5.33 (m, 3H, H_3, H_{15}, H_{19}), 4.55-4.70 (m, 2H, 2 x H_{8a}), 4.42-4.44 (m, 1H, H_5), 4.09 (s, 1H, C_7-OH, D_2O exchangeable), 4.00 (s, 1H, H_{13}), 3.81 (d, 1H, J = 4 Hz, H_6), 3.63-3.71 (m, 1H, H_{17}), 3.34-3.36 (m, 1H, H_2), 3.19 (dd, 1H, H_{25}), 2.48-2.56 (m, 1H, H_{12}), 2.22-2.34 (m, 3H, 2 x H_{16}, H_{26}), 2.00 (dd, 1H, H_{18a}), 1.78 (s, 3H, 3 x H_{4a}), 1.72 (dt, 1H, H_{20a}), 1.29-1.75 (m, 11H, 3 x H_{14a}, H_{20b}, 2 x H_{22}, 2 x H_{23}, 2 x H_{27}, C_{13}-OH, D_2O exchangeable), 1.17 (d, 3H, J = 8 Hz, 3 x H_{12a}), 0.95 (t, 3H, J = 4 Hz, 3 x H_{28a}), 0.92 (s, 9H, -C($\underline{CH_3}$)$_3$), 0.79-0.86 (m, 7H, H_{18b}, 3 x

H_{26a}, 3 x H_{24a}), 0.13 (s, 6H, -Si($\underline{CH_3}$)$_2$). ^{13}C NMR (100 MHz, $CDCl_3$, 25 °C): δ (ppm) 173.87, 140.37, 138.80, 137.38, 136.62, 124.90, 119.43, 117.45, 117.20, 97.53, 80.18, 80.15, 77.72, 77.33, 69.52, 68.73, 68.02, 67.31, 45.81, 41.42, 40.02, 36.74, 35.87, 35.58, 34.33, 31.33, 28.16, 27.57, 25.97, 20.13, 19.35, 18.51, 17.55, 14.75, 12.65, 11.83, -4.51, -4.77. HRMS: *m/z* $[M+Na]^+$ for $C_{40}H_{64}O_8Si$, calculated 723.4263; observed 723.4454.

Synthesis of (6). To an ice cooled solution of **5** (0.5 g, 0.7 mmol), triethylamine (0.14 g, 1.4 mmol) and DMAP (0.001 g, 0.01 mmol) in dry DCM (15 ml) a solution of chloroacetyl chloride in dry DCM (5 ml) was added. The resulting brown solution was stirred at room temperature for 3 h and the reaction mixture was poured into water and extracted with DCM (2×20 ml). The combined organic extract was treated with dilute hydrochloric acid (2×10 ml, 5%, *v/v*), neutralized with aqueous sodium bicarbonate solution (2×10 ml, 5%, *w/v*) and washed with saturated sodium chloride solution (2×10 ml). After drying the extract over anhydrous sodium sulfate, solvent was removed under reduced pressure to isolate the crude product, which was purified by column chromatography over silica gel (60-120 mesh) using hexane/ethyl acetate (92:8, *v/v*) as eluent to obtain **6** (0.39 g, 70.9 %) as a white amorphous solid. IR: ν_{max} 3451.5, 2929.7, 2363.1, 1736.9, 1146.1, 1379.1, 1252.4, 1170.4, 1073.5, 991.5, 492.0 cm^{-1}. ^{1}H NMR (400 MHz, $CDCl_3$, 25 °C): δ (ppm) 5.76-5.89 (m, 2H, H_9, H_{10}), 5.63-5.72 (m, 1H, H_{11}), 5.26-5.38 (m, 2H, H_3, H_{19}), 5.22 (s, 1H, H_{13}), 5.02-5.10 (m, 1H, H_{15}), 4.54-4.75 (m, 2H, 2 x H_{8a}), 4.40-4.49 (m, 1H, H_5), 4.13-4.22 (m, 3H, -CH_2-Cl, C_7-OH, D_2O exchanged), 3.83 (d, 1H, J = 4 Hz, H_6), 3.65 (m, 1H, H_{17}), 3.38 (dd, 1H, H_2), 3.20 (d, 1H, J = 4 Hz, H_{25}), 2.63-2.74 (m, 1H, H_{12}), 2.21-2.36 (m, 3H, 2 x H_{16}, H_{26}), 2.00-2.03 (m, 1H, H_{18a}), 1.81 (s, 3H, 3 x H_{4a}), 1.24-1.74 (m, 12H, 3 x H_{14a}, 2 x H_{20}, 2 x H_{22}, 2 x H_{23}, H_{24}, 2 x H_{27}), 1.08 (d, 3H, J = 8 Hz, 3 x H_{12a}), 0.92-0.98 (m, 12H, 3 x H_{28}, -C($\underline{CH_3}$)$_3$), 0.74-0.83 (m, 4H, 3 x H_{26a}, H_{18b}), 0.51 (s, 6H, -Si($\underline{CH_3}$)$_2$). ^{13}C

NMR (100 MHz, $CDCl_3$, 25 °C): δ (ppm) 174.17, 166.59, 140.44, 137.49, 135.67, 133.87, 125.71, 119.04, 118.24, 117.33, 97.57, 80.63, 80.24, 80.12, 77.33, 77.04, 69.49, 68.75, 67.96, 67.05, 45.76, 41.31, 40.88, 39.11, 36.79, 35.80, 35.54, 34.23, 30.29, 28.12, 27.44, 26.98, 25.96, 20.13, 18.90, 18.50, 17.53, 14.72, 12.61, 12.02, -4.51, -4.77. HRMS: *m/z* $[M+K]^+$ for $C_{42}H_{65}ClO_9Si$, calculated 815.3718; observed 815.3767.

Synthesis of (7). Chloroacetylated ivermectin aglycon **6** (0.3 g, 0.3 mmol) was dissolved in dry DMF (7 ml) and NaN_3 (0.04 g, 0.6 mmol) was added and the reaction mixture was heated at 60 °C for 24 h. After completion of reaction, DMF was removed under reduced pressure. The residue was dissolved in ethyl acetate (80 ml) and the solution was washed with water (3 × 30 ml). After drying with anhydrous sodium sulfate, solvent was removed. The light brown residue was extracted in hexanes. Evaporation of hexane on a rotavap yielded **7**, which was used as such in subsequent reactions.

Synthesis of (8) and (9). Compounds **8** and **9** were synthesized following the reported procedures,[64] and the characteristic data of compounds is given below.

Ethynylferrocene (8). Orange solid. Yield: 72%. IR: ν_{max} 3280, 3105, 3089, 2924, 2854, 2104, 1639, 1443, 1022 cm^{-1}. ^1H NMR (500 MHz, $CDCl_3$): δ (ppm) 4.45 (s, 2H, Cp ring), 4.21 (s, 5H, Cp ring), 4.19 (s, 2H, Cp ring), 2.72 (s, 1H, -CH) and ^{13}C NMR (125 MHz, $CDCl_3$): δ (ppm) 71.77, 70.07, 68.74, 63.87. Anal. Calcd. for $C_{12}H_{10}Fe$: C,68.62; H, 4.80. Found: C, 68.66; H, 4.82.

4-(Ethynylphenyl)ferrocene (9). Orange solid. Yield: 65%. IR: ν_{max} 3286, 3088, 2924, 2104, 1667, 1604, 1523, 1435,1027 cm^{-1}. ^1H NMR (500 MHz, $CDCl_3$): δ (ppm) 3.10 (s, 1H, -CH), 4.00 (s, 5H, Cp ring), 4.35 (s, 2H, Cp ring), 4.65 (s, 2H, Cp ring,), 7.44-7.56 (m, 4H, $-C_6H_5$). ^{13}C

NMR (125 MHz, $CDCl_3$): δ (ppm) 140.47, 132.15, 126.38, 125.77, 84.09, 84.01, 69.72, 69.39, 66.56. Anal. Calcd. for $C_{18}H_{14}Fe$: C, 75.55;H, 4.93. Found: C, 75.54; H, 4.91.

General procedure for the synthesis of (10a-c). Alkynes **10a-c** were prepared using a modified procedure,[38] To a solution of appropriate alkyl 2-chloro-4-methyl-6-arylpyrimidin-5-carboxylate (0.5 g, 2.56 mmol) in dry CH_3CN (20 ml), dry K_2CO_3 (1.06 g, 7.69 mmol) and propargyl alcohol (0.2 ml, 3.84 mmol) were added and the reaction mixture was refluxed overnight. After the completion of the reaction, CH_3CN was removed under vacuum. Water was then added to the residue and the product was extracted with DCM (2×20 ml). Solvent was removed to obtain crude, which was purified by column chromatography over silica (60-120 mesh) using hexane/ethyl acetate as eluent to isolate analytically pure **10a-c**.

Isopropyl 4-methyl-6-(3-nitrophenyl)-2-(prop-2-yn-1-yloxy)pyrimidine-5-carboxylate (10a). Chromatographic eluent: hexane/ethyl acetate (70:30 *v/v*). White solid. Yield: 94%. IR: ν_{max} 3272.6, 3071.3, 2989.3, 2288.6, 1714.6, 1528.2, 1416.4, 1341.8, 1252.4, 1170.4, 1058.6, 909.5, 842.4, 670.9 cm^{-1}. ^1H NMR (300 MHz, $CDCl_3$, 25 °C): δ (ppm) 8.55 (s, 1H, ArH), 8.34 (d, 1H, 6Hz, ArH), 8.03 (d, 1H, 6Hz, ArH), 7.63-7.67 (m, 1H, ArH), 5.09-5.29 (m, 3H, $-OCH_2-$, $-O\underline{CH}(CH_3)_3$), 2.50-2.66 (m, 4H, $-CH_3$, -CH), 1.17 (d, 6H, $-CH(\underline{CH_3})_2$). ^{13}C NMR (75 MHz, $CDCl_3$, 25 °C): δ (ppm) 169.65, 166.93, 163.56, 163.17, 148.20, 139.02, 134.50, 129.63, 124.83, 123.59, 121.04, 77.92, 75.02, 70.20, 55.32, 22.78, 21.24. *m/z* $[M+H]^+$ for $C_{18}H_{17}N_3O_5$, calculated 356.1312; observed 356.1240.

Ethyl 4-methyl-6-(2-nitro-4,5-dimethoxyphenyl)-2-(prop-2-yn-1-yloxy)pyrimidine-5-carboxylate (10b). Chromatographic eluent: hexane/ethyl acetate (55:45 *v/v*). White solid. Yield: 92%. IR: ν_{max} 3295.0, 2987.0, 2847.7, 1714.6, 1520.8, 1446.2, 1341.8, 1274.7, 1058.6, 775.3 cm^{-1}. ^1H NMR (300 MHz, $CDCl_3$, 25 °C): δ (ppm) 7.71 (s, 1H, ArH), 6.71 (s, 1H, ArH),

5.02 (s, 2H, -OCH_2-), 4.04-4.09 (m, 2H, -$\underline{CH_2}CH_3$), 3.99 (s, 3H, -OCH_3), 3.91 (s, 3H, -OCH_3), 2.66 (s, 3H, -CH_3), 2.46 (s, 1H, CCH), 1.01 (t, 3H, -$CH_2\underline{CH_3}$). ^{13}C NMR (75 MHz, $CDCl_3$, 25 °C): δ (ppm) 170.45, 167.00, 166.00, 163.01, 153.00, 149.10, 139.95, 128.20, 119.60, 111.53, 107.22, 77.88, 74.95, 61.43, 56.50, 55.35, 23.78, 12.56. HRMS: *m/z* $[M+H]^+$ for $C_{19}H_{19}N_3O_7$, calculated 402.1170; observed 402.1379.

Ethyl 4-methyl-6-phenyl-2-(prop-2-yn-1-yloxy)pyrimidine-5-carboxylate (10c). Chromatographic eluent: hexane/ethyl acetate (90:10 *v/v*). White solid, Yield: 94%. IR: ν_{max} 1533, 1552, 1708, 2985, 3250, 2985, 1708, 1552, 1533 cm^{-1}. ^{1}H NMR (500 MHz, $CDCl_3$, 25 °C): δ (ppm) 7.44-7.69 (m, 5H, ArH), 5.11 (d, 2H, J = 2.5 Hz, -OCH_2-), 4.18 (q, 2H, J = 10 Hz, -$O\underline{CH_2}CH_3$), 2.61 (s, 3H, -CH_3), 2.5 (t, 1H, J = 2.5 Hz, -CCH), 1.07 (t, 3H, J = 5 Hz, -$OCH_2\underline{CH_3}$). ^{13}C NMR (125 MHz, $CDCl_3$, 25 °C): δ (ppm) 13.62, 22.77, 55.15, 61.75, 74.76, 78.29, 120.53, 128.36, 128.43, 130.25, 137.54, 163.06, 166.36, 168.13, 168.97. HRMS: *m/z* $[M]^+$for $C_{17}H_{16}N_2O_3$, calculated 296.1161; observed 296.1489.

General procedure for the synthesis of (11-15). To a solution of **7** (0.100 g, 1.2 mmol) and appropriate alkyne derivative **8-10** (1.2 mmol) in EtOH: H_2O (10 ml, 8:2, *v/v*), $CuSO_4$.5 H_2O (0.011 g, 0.07 mmol) and sodium-(L)-ascorbate (0.06 g, 0.3 mmol) were added. The reaction mixture was stirred at room temperature for 12-16 h. After completion of reaction, solvent was removed under vacuum. Water was added to the residue and the product was extracted with DCM (50 ml). The organic layer was dried over anhydrous sodium sulfate, subsequently solvent was removed under vacuum to obtain crude product which was further purified by column chromatography over silica (60-120 mesh) using hexane/ethyl acetate as eluent to obtain pure compounds. Characteristic data of the compounds isolated using this procedure is given below.

5-O-(tert-Butyldimethylsilyl)-(4-(ferrocenyl)-1H-1,2,3-triazol-1-yl) (ivermectin aglycon-13-O-yl)-2-acetate (11). Chromatographic eluent: hexane/ethyl acetate (80:20, *v/v*). Orange solid, Yield: 61 %. IR: ν_{max} 3503.7, 2929.7, 2862.6, 1751.8, 1699.7, 1461.1, 1371.7, 1252.4, 1192.7, 1073.5, 991.6, 805.1 cm^{-1}. ^1H NMR (500 MHz, $CDCl_3$, 25 °C): δ (ppm) 7.61 (s, 1H, triazole CH), 6.11-6.15 (m, 2H, H_9, -CHCOH), 5.73-5.82 (m, 2H, H_{10}, H_{11}), 5.26-5.33 (m, 3H, H_3, H_{13}, H_{19}), 4.97 (d, 1H, J = 10 Hz, H_{15}), 4.80 (s, 1H, -CHCOH, D_2O exchangeable), 4.73 (s, 2H, cp ring), 4.47-4.58 (m, 2H, 2 x H_{8a}), 4.29 (s, 2H, cp ring), 4.08-4.13 (m, 1H, H_5), 4.07 (s, 5H, cp ring), 3.94 (br, 1H, H_6), 3.58 (m, 2H, H_{17}, H_{25}), 3.21 (d, 1H, J = 10 Hz, H_2), 2.60-2.65 (m, 2H, H_{12}, H_{24}), 2.19-2.32 (m, 3H, 2 x H_{16}, H_{26}), 1.82-1.95 (d, 1H, J = 15 Hz, H_{18b}), 1.81-1.83 (m, 1H, H_{20a}), 1.66 (d, 1H, J = 15 Hz, H_{20b}), 1.48-1.57 (m, 6H, 2 x H_{22}, 2 x H_{23}, 2 x H_{27}), 1.41 (s, 3H, 3 x H_{4a}), 1.13 (d, 3H, J = 10 Hz, 3 x H_{14a}), 1.05 (d, 3H, J = 10 Hz, 3 x H_{12a}), 0.98 (t, 3H, J = 5 Hz, 3 x H_{28}), 0.92 (s, 9H, -C(CH_3)$_3$), 0.83-0.85 (m, 3H, 3 x H_{24a}), 0.79 (d, 3H, J = 5 Hz, 3 x H_{26a}), 0.68-0.76 (m, 1H, H_{18a}), 0.11 (s, 6H, -Si(CH_3)$_2$). ^{13}C NMR (125 MHz, $CDCl_3$, 25 °C): δ (ppm) 168.8, 165.69, 147.45, 140.63, 139.47, 135.34, 133.60, 129.44, 126.71, 121.98, 120.09, 118.14, 97.40, 83.19, 81.11, 78.86, 75.01, 73.36, 69.57, 68.15, 66.90, 66.76, 66.73, 60.37, 50.62, 40.49, 38.98, 36.81, 35.86, 35.53, 34.50, 32.97, 27.96, 27.42, 26.91, 25.96, 25.91, 18.49, 18.20, 17.46, 17.15, 14.66, 12.70, 11.80, -4.27, -4.63. HRMS: *m/z* $[M]^+$ for $C_{54}H_{75}FeN_3O_9Si$, calculated 993.4618; observed 993.3912.

5-O-(tert-Butyldimethylsilyl)-(4-(4-ferrocenylphenyl)-1H-1,2,3-triazol-1-yl)(ivermectin aglycon-13-O-yl)-2-acetate (12). Chromatographic eluent: hexane/ethyl acetate (80:20, *v/v*). Orange solid. Yield: 59%. IR: ν_{max} 3488.8, 2929.7, 2862.6, 1751.8, 1699.7, 1461.1, 1379.1, 1252.4, 1192.7, 1073.5, 991.5, 805.1 cm^{-1}. ^1H NMR (500 MHz, $CDCl_3$, 25 °C): δ (ppm) 7.92 (s, 1H, triazole CH), 7.77 (d, 2H, J = 10 Hz, ArH), 7.54 (d, 2H, J = 10 Hz, ArH), 6.13-6.16 (m, 2H,

H_9, -CHCOH), 5.63-5.80 (m, 2H, H_{10}, H_{11}), 5.24-5.35 (m, 3H, H_3, H_{13}, H_{19}), 4.98 (d, 1H, J = 10 Hz, H_{15}), 4.82 (s, 1H, -CHCOH, D_2O exchangeable), 4.68 (s, 2H, cp ring), 4.49-4.59 (m, 2H, 2 x H_{8a}), 4.34 (s, 2H, cp ring), 4.0-4.16 (m, 1H, H_5), 4.06 (s, 5H, cp ring), 3.96 (br, 1H, H_6), 3.67-3.74 (m, 2H, H_{17}, H_{25}), 3.22 (d, 1H, J = 10 Hz, H_2), 2.62-2.66 (m, 2H, H_{12}, H_{24}), 2.20-2.34 (m, 3H, 2 x H_{16}, H_{26}), 1.93-1.96 (m, 1H, H_{18b}), 1.83 (d, 1H, J = 10 Hz, H_{20a}), 1.42-1.69 (m, 10H, 3 x H_{4a}, H_{20b}, 2 x H_{22}, 2 x H_{23}, 2 x H_{27}), 1.14 (d, 3H, J = 10 Hz, 3 x H_{14a}), 1.06 (d, 3H, J = 5 Hz, 3 x H_{12a}), 0.99 (t, 3H, J = 10 Hz, 3 x H_{28}), 0.93 (s, 9H, -C(CH_3)$_3$), 0.84-0.86 (m, 3H, 3 x H_{24a}), 0.80 (d, 3H, J = 5 Hz, 3 x H_{26a}), 0.69-0.76 (m, 1H, H_{18a}), 0.12 (s, 6H, -Si(CH_3)$_2$-). ^{13}C NMR (125 MHz, $CDCl_3$, 25 °C): δ (ppm) 168.88, 165.55, 148.53, 140.62, 139.64, 139.49, 135.37, 133.58, 129.44, 127.82, 126.71, 126.45, 128.58, 122.01, 120.66, 118.17, 97.52, 83.20, 81.18, 78.87, 73.36, 69.68, 69.12, 68.78, 68.17, 66.91, 66.50, 66.49, 60.40, 50.76, 40.49, 38.98, 36.82, 35.87, 35.54, 34.50, 32.97, 31.93, 29.70, 27.44, 25.92, 18.90, 18.22, 17.47, 17.16, 14.68, 12.70, 11.82, -4.26, -4.62. HRMS: *m/z* $[M]^+$ for $C_{60}H_{79}FeN_3O_9Si$, calculated 1069.4929; observed 1069.4765.

Isopropyl 4-methyl-6-(3-nitrophenyl)-2-((1-(2-oxo-2-(5-O-(tert-butyldimethylsilyl)-ivermectin aglycon-13-O-yloxy)ethyl)-1H-1,2,3-triazol-4-yl)methoxy)pyrimidine-5-carboxylate (13). Chromatographic eluent: hexane/ethyl acetate (55:45, *v/v*). White Solid. Yield: 62%. IR: ν_{max} 3498.1, 2961.4, 2929.7, 2871.9, 1718.3, 1750.0, 1531.9, 1467.4, 1349.3, 1261.7, 1049.2, 989.6 cm^{-1}. ^{1}H NMR (500 MHz, $CDCl_3$, 25 °C): δ (ppm) 8.51 (s, 1H, ArH), 8.33 (d, 1H, J = 10 Hz, ArH), 8.02 (d, 1H, J = 10 Hz, 1H, ArH) 7.88 (s, 1H, triazole CH), 7.64 (t, 1H, J = 10 Hz, ArH), 6.12-6.16 (m, 2H, H_9, -CHCOH), 5.63-5.79 (m, 4H, H_{10}, H_{11}, -OCH_2-), 5.22-5.34 (m, 3H, H_3, H_{13}, H_{19}), 5.12-5.14 (m, 1H, -CH(CH_3)$_2$), 4.95 (d, 1H, J = 10 Hz, H_{15}), 4.80 (s, 1H, -CHCOH, D_2O exchangeable), 4.48-4.58 (m, 2H, 2 x H_{8a}), 4.10-4.14 (m, 1H, H_5), 3.95 (br, 1H, H_6), 3.66-3.73 (m, 2H, H_{17}, H_{25}), 3.21 (d, 1H, J = 5 Hz, H_2), 2.62-2.65 (m, 2H, H_{12}, H_{24}), 2.21-

2.33 (m, 3H, 2 x H_{16}, H_{26}), 1.93 (d, 1H, J = 10 Hz, H_{18b}), 1.82 (d, 1H, J = 15 Hz, H_{20a}), 1.39-1.68 (m, 10H, 3 x H_{4a}, H_{20b}, 2 x H_{22}, 2 x H_{23}, 2 x H_{27}), 1.14-1.17 (m, 9H, -CH($\underline{CH_3}$)$_2$, 3 x H_{14a}), 1.04 (d, 3H, J = 15 Hz, 3 x H_{12a}), 0.93-0.97 (m, 12H, 3 x H_{28}, -C($\underline{CH_3}$)$_3$), 0.83 (d, 3H, J = 5 Hz, 3 x H_{24a}), 0.80 (d, 3H, J = 5 Hz, 3 x H_{26a}), 0.67-0.72 (m, 1H, H_{18a}), 0.12 (s, 6H, -Si($\underline{CH_3}$)$_2$-). ^{13}C NMR (125 MHz, $CDCl_3$, 25 °C): δ (ppm) 169.54, 168.78, 166.86, 165.43, 163.72, 163.61, 148.21, 143.84, 140.64, 139.48, 139.20, 135.34, 134.48, 133.48, 129.58, 129.48, 126.71, 126.69, 124.69, 123.53, 122.00, 120.91, 118.24, 97.39, 83.22, 81.19, 78.86, 73.38, 70.19, 68.81, 68.13, 66.88, 61.41, 50.64, 40.51, 38.98, 36.82, 35.88, 35.54, 34.47, 32.98, 31.28, 29.68, 27.97, 27.43, 25.94, 25.90, 22.91, 21.38, 18.84, 18.20, 17.42, 17.13, 14.63, 12.64, 11.76, -4.28, -4.64. HRMS: *m/z* $[M+Na]^+$ for $C_{60}H_{82}N_6O_{14}Si$, calculated 1161.5550; observed 1161.5581.

Ethyl 4-methyl-6-(2-nitro-4,5-dimethoxyphenyl)-2-((1-(2-oxo-2-(5-O-(tert-butyldimethylsilyl)-ivermectin aglycon-13-O-yloxy)ethyl)-1H-1,2,3-triazol-4-yl)methoxy)pyrimidine-5-carboxylate (14). Chromatographic eluent: hexane/ethyl acetate (65:35, *v/v*). White Solid. Yield: 62%. IR: ν_{max} 3660.2, 3414.2, 2929.7, 2360.7, 1729.5, 1505.8, 1453.7, 1334.4, 1244.9, 1155.5, 1058.6 cm^{-1}. ^{1}H NMR (400 MHz, $CDCl_3$, 25 °C): δ (ppm) 7.78 (s, 1H, triazole CH), 7.70 (s, 1H, ArH), 6.71 (s, 1H, ArH), 6.10-6.15 (m, 2H, H_9, -$\underline{CH}$COH), 5.62-5.78 (m, 4H, H_{10}, H_{11}, -O$\underline{CH_2}$-), 5.21-5.33 (m, 3H, H_3, H_{13}, H_{19}), 4.94 (d, 1H, H_{15}), 4.81 (s, 1H, -CHC$\underline{OH}$, D_2O exchangeable), 4.46-4.58 (m, 2H, 2 x H_{8a}), 3.92-4.14 (m, 10H, H_5, H_6, -OCH_3, -OCH_3, -$\underline{CH_2}CH_3$), 3.65-3.71 (m, 2H, H_{17}, H_{25}), 3.19 (br, 1H, H_2), 2.60-2.66 (m, 5H, H_{12}, H_{24}, -CH_3), 2.16-2.31 (m, 3H, 2 x H_{16}, H_{26}), 1.90-1.94 (m, 1H, H_{18b}), 1.80 (d, 1H, H_{20a}), 1.47-1.67 (m, 10H, 3 x H_{4a}, H_{20b}, 2 x H_{22}, 2 x H_{23}, 2 x H_{27}), 0.89-1.04 (m, 18H, 3 x H_{12a}, 3 x H_{28}, -$OCH_2\underline{CH_3}$, -C(CH_3)$_3$), 0.65-0.83 (m, 7H, 3 x H_{26a}, 3 x H_{24a}, H_{18a}), 0.11 (s, 6H, -Si($\underline{CH_3}$)$_2$-). ^{13}C NMR (100 MHz,$CDCl_3$, 25 °C): δ (ppm) 170.62, 168.85, 166.99, 166.07, 165.60, 163.48,

153.15, 149.13, 143.79, 140.58, 139.91, 139.56, 135.51, 133.59, 129.47, 128.47, 126.71, 124.95, 122.08, 119.47, 118.18, 111.66, 97.44, 83.26, 81.14, 78.91, 73.40, 68.86, 68.24, 66.93, 61.58, 61.47, 56.75, 56.62, 50.63, 40.54, 39.03, 36.85, 35.93, 35.56, 34.55, 33.02, 31.34, 27.97, 28.02, 27.49, 25.03, 25.98, 24.04, 18.92, 18.28, 17.51, 17.23, 14.72, 13.83, 12.76, 11.80, -4.20, -4.56. HRMS: *m/z* $[M+Na]^+$ for $C_{61}H_{84}N_6O_{16}Si$, calculated 1207.5605; observed 1207.5608.

Ethyl 4-methyl-6-(phenyl)-2-((1-(2-oxo-2-(5-O-(tert-butyldimethylsilyl)-ivermectin aglycon-13-O-yloxy)ethyl)-1H-1,2,3-triazol-4-yl)methoxy)pyrimidine-5-carboxylate (15). Chromatographic eluent: hexane/ethyl acetate (70:30, *v/v*). White Solid. Yield: 57 %. IR: ν_{max} 3496.2, 2929.7, 2325.9, 1722.0, 1550.6, 1453.7, 1364.2, 1252.4, 1073.5, ^{1}H NMR (400 MHz, $CDCl_3$, 25 °C): δ (ppm) 7.84 (s, 1H, triazole CH), 7.63 (dd, 2H, ArH), 7.41-7.48 (m, 3H, ArH), 6.12-6.16 (m, 2H, H_9, -<u>CH</u>COH), 5.61-5.76 (m, 4H, H_{10}, H_{11}, -O<u>CH_2</u>-), 5.25-5.33 (m, 3H, H_3, H_{13}, H_{19}), 4.94 (d, 1H, H_{15}), 4.83 (s, 1H, -CHC<u>OH</u>, D_2O exchangeable), 4.47-4.59 (m, 2H, 2 x H_{8a}), 4.12-4.18 (m, 3H, H_5, -O<u>CH_2</u>CH_3), 3.94-3.99 (br, 1H, H_6), 3.65-3.72 (m, 2H, H_{17}, H_{25}), 3.20 (d, 1H, H_2), 2.60-2.66 (m, 2H, H_{12}, H_{24}), 2.58 (s, 3H, -CH_3), 2.17-2.32 (m, 2H, 2 x H_{16}), 1.94 (dd, 1H, H_{18b}), 1.81 (d, 1H, H_{20a}), 1.48-1.67 (m, 10H, 3 x H_{4a}, H_{20b}, 2 x H_{22}, 2 x H_{23}, 2 x H_{27}), 1.01-1.06 (m, 6H, 3 x H_{12a}, -OCH_2<u>CH_3</u>), 0.90-0.97 (m, 12H, 3 x H_{28}, -$C(CH_3)_3$), 0.66-0.83 (m, 7H, 3 x H_{26a}, 3 x H_{24a}, H_{18a}), 0.12 (s, 6H, -Si(<u>CH_3</u>)$_2$-). ^{13}C NMR (400 MHz,$CDCl_3$, 25 °C): δ (ppm) 169.02, 168.87, 168.27, 166.62, 165.57, 163.57, 144.23, 140.58, 139.59, 137.64, 135.49, 133.62, 130.31, 129.44, 128.54, 128.40, 126.72, 124.72, 122.09, 120.43, 118.13, 97.45, 83.25, 81.17, 78.91, 73.39, 68.88, 68.26, 66.92, 61.83, 61.35, 50.66, 40.53, 39.01, 36.84, 35.93, 35.55, 34.54, 33.02, 31.35, 28.01, 27.90, 26.04, 25.99, 22.89, 18.95, 18.30, 17.53, 17.24, 14.75, 13.70, 12.80, 11.81, -4.20, -4.55. HRMS: *m/z* $[M+Na]^+$for $C_{59}H_{81}N_5O_{12}Si$, calculated 1102.5543 ; observed 1102.5580.

General procedure for the synthesis of (16-20). To a solution of **11-15** (0.2 g) in methanol (10 ml), a solution of *p*-toulenesulfonic acid-methanol (10 ml, 0.02 g ml $^{-1}$) was added dropwise. The reaction mixture was stirred at room temperature for 45 min. After the completion of the reaction, the reaction mixture was partitioned between dichloromethane (30 ml) and aqueous sodium bicarbonate solution (5%, *w/v*). Organic layer was washed with saturated sodium chloride solution (2 × 20 ml), dried over sodium sulfate and concentrated under reduced pressure. The resulting residue was purified by column chromatography over silica gel (60-120 mesh) using hexane/ethyl acetate as eluent. Characteristic data of the compounds synthesized using this procedure is given below.

13-O-(4-(Ferrocenyl)-1H-1,2,3-triazol-1-yl-2-acetate) ivermectin aglycon (16). Chromatographic eluent: Hexane/ethyl acetate (45:55, *v/v*). Orange Solid. mp, 74 ºC. Yield: 78%. Rf: (0.3, 55 % ethyl acetate/hexane). IR: ν_{max} 3414.2, 2922.2, 1751.8, 1699.7, 1461.1, 1379.1, 1207.7, 1051.1, 991.5, 820.0 cm^{-1}. ^{1}H NMR (500 MHz , $CDCl_3$): δ (ppm) 7.58 (s, 1H, triazole CH), 6.16-6.18 (m, 2H, H_9, -<u>CH</u>COH), 5.64-5.80 (m, 2H, H_{10}, H_{11}), 5.24-5.34 (m, 4H, H_3, H_5, H_{13}, H_{19}), 5.00 (d, 1H, J = 10 Hz, H_{15}), 4.81-4.82 (m, 3H, cp ring, -CHC<u>OH</u>, D_2O exchangeable), 4.50-4.59 (m, 2H, 2 x H_{8a}), 4.37 (s, 2H, cp ring), 4.14 (s, 5H, cp ring), 4.06 (br, 1H, H_6), 3.70-3.74 (m, 1H, H_{17}), 3.60 (m, 1H, H_{25}), 3.22 (d, 1H, J = 10 Hz, H_2), 2.65-2.66 (m, 1H, H_{12}), 2.50-2.52 (m, 1H, H_{24}), 2.17-2.33 (m, 2H, 2 x H_{16}), 1.95 (d, 1H, J = 10 Hz, H_{18b}), 1.82-1.87 (m, 2H, H_{20a}, H_{26}), 1.42-1.69 (m, 10H, 3 x H_{4a}, H_{20b}, 2 x H_{22}, 2 x H_{23}, 2 x H_{27}), 1.23 (d, 3H, J = 10 Hz, 3 x H_{14a}), 1.06 (d, 3H, J = 5 Hz, 3 x H_{12a}), 0.99 (t, 3H, 3 x H_{28}), 0.85 (d, 3H, J = 15 Hz, 3 x H_{24a}), 0.80 (br, 3H, 3 x H_{26a}), 0.69-0.73 (m, 1H, H_{18a}). ^{13}C NMR (125 MHz, $CDCl_3$, 25 °C): δ (ppm) 168.88, 165.70, 147.79, 140.52, 138.83, 135.63, 133.59, 129.64, 126.63, 122.30, 120.10, 118.10, 97.39, 82.85, 81.01, 78.51, 72.26, 69.67, 68.81, 68.16, 66.78, 50.61, 40.48,

38.93, 36.82, 35.82, 35.50, 34.49, 33.32, 31.26, 29.69, 27.92, 27.42, 18.85, 17.45, 16.88, 14.62, 12.72, 12.32, 11.77. HRMS: *m/z* $[M]^+$ for $C_{48}H_{61}FeN_3O_9$, calculated 879.3757; observed 879.3765. t_R (245 nm) = 13.30 min.

13-O-(4-(Ferrocenylphenyl)-1H-1,2,3-triazol-1-yl-2-acetate) ivermectin aglycon (17). Chromatographic eluent: Hexane/ethyl acetate (45:55, *v/v*). Orange Solid. mp, 192 ºC. Yield: 78%. IR: ν_{max} 3481.3, 2922.2, 1751.8, 1699.7, 1453.7, 1371.7, 1259.8, 1192.7, 1051.1, 991.5, 805.1 cm^{-1}. ^1H NMR (500 MHz, $CDCl_3$, 25 °C): δ (ppm) 7.91 (s, 1H, triazole CH), 7.75 (d, 2H, *J* = 10 Hz, ArH), 7.48 (br doublet, 1H, ArH), 6.16 (m, 2H, H_9, -CHCOH), 5.64-5.82 (m, 2H, H_{10}, H_{11}), 5.25-5.38 (m, 4H, H_3, H_5, H_{13}, H_{19}), 4.99 (d, 1H, *J* = 10 Hz, H_{15}), 4.83 (s, -CHCOH, D_2O exchangeable), 4.78 (s, 2H, cp ring), 4.50-4.59 (m, 2H, 2 x H_{8a}), 4.43 (s, 2H, cp ring), 4.13 (s, 5H, cp ring), 4.06 (br, 1H, H_6), 3.70-3.74 (m, 1H, H_{17}), 3.58-3.62 (m, 1H, H_{25}), 3.22 (d, 1H, *J* = 5 Hz, H_2), 2.64-2.67 (m, 1H, H_{12}), 2.50-2.53 (m, 1H, H_{24}), 2.20-2.34 (m, 2H, 2 x H_{16}), 1.94-1.96 (m, 1H, H_{18b}), 1.81-1.89 (m, 2H, H_{20a}, H_{26}), 1.42-1.69 (m, 10H, 3 x H_{4a}, H_{20b}, 2 x H_{22}, 2 x H_{23}, 2 x H_{27}), 1.23 (d, 3H, *J* = 5 Hz, 3 x H_{14a}), 1.06 (d, 3H, *J* = 5 Hz, 3 x H_{12a}), 0.99 (t, 3H, 3 x H_{28}), 0.85 (d, 3H, *J* = 5 Hz, 3 x H_{24a}), 0.80 (br, 3H, 3 x H_{26a}), 0.69-0.73 (m, 1H, H_{18a}). ^{13}C NMR (125 MHz, $CDCl_3$, 25 °C): δ (ppm) 168.66, 165.61, 148.42, 140.52, 139.62, 138.80, 135.63, 133.56, 129.65, 127.79, 126.62, 126.44, 125.81, 122.31, 120.57, 118.1, 97.39, 82.83, 81.05, 78.50, 72.27, 69.90, 69.35, 68.81, 68.16, 66.85, 66.61, 50.74, 40.48, 38.94, 36.82, 35.83, 35.50, 34.48, 33.34, 31.26, 27.93, 27.43, 18.85, 17.47, 16.87, 14.63, 12.72, 11.78. HRMS: *m/z* $[M]^+$ for $C_{54}H_{65}FeN_3O_9$, calculated 955.4070; observed 955.4152.

Isopropyl 4-methyl-6-(3-nitrophenyl)-2-((1-(2-oxo-2-(ivermectin aglycon-13-O-yloxy)ethyl)-1H-1,2,3-triazol-4-yl)methoxy)pyrimidine-5-carboxylate (18). Chromatographic eluent: Hexane/ethyl acetate (25:75, *v/v*). White solid. mp, 97 ºC. Yield: 81 %, IR: ν_{max} 3503.7,

2929.7, 2877.5, 1714.6, 1593.4, 1535.7, 1453.7, 1349.3, 1259.8, 1058.6, 991.5, 805.1 cm^{-1}. ^{1}H NMR (500 MHz, $CDCl_3$, 25 °C): δ (ppm) 8.51 (s, 1H, ArH), 8.33 (d, 1H, J = 10 Hz, ArH), 8.02 (d, 1H, J = 10 Hz, ArH), 7.88 (s, 1H, triazole CH), 7.64 (t, 1H, J = 10 Hz, ArH), 6.16-6.18 (m, 2H, H_9, -CHCOH), 5.62-5.79 (m, 4H, H_{10}, H_{11}, -OCH_2-), 5.22-5.35 (m, 4H, H_3, H_5, H_{13}, H_{19}), 5.11-5.15 (m, 1H, -OCH$(CH_3)_2$), 4.96 (d, 1H, J = 10 Hz, H_{15}), 4.82 (s, 1H, -CHCOH, D_2O exchangeable), 4.49-4.59 (m, 2H, 2 x H_{8a}), 4.06 (s, 1H, H_6), 3.69-3.73 (m, 1H, H_{17}), 3.59 (d, 1H, J = 10 Hz, H_{25}), 3.21 (d, 1H, J = 5 Hz, H_2), 2.62-2.65 (m, 4H, H_{12}, -CH_3), 2.49-2.54 (m, 1H, H_{24}), 2.18-2.33 (m, 2H, 2 x H_{16}), 1.93-1.95 (m, 1H, H_{18b}), 1.81-1.88 (m, 2H, H_{20a}, H_{26}), 1.38-1.72 (m, 10H, 3 x H_{4a}, H_{20b}, 2 x H_{22}, 2 x H_{23}, 2 x H_{27}), 1.21 (d, 3H, J = 5 Hz, 3 x H_{14a}), 1.16 (d, 6H, J = 5 Hz,-CH(CH_3)$_3$), 1.05 (d, 3H, J = 10 Hz, 3 x H_{12a}), 0.97 (t, 3H, 3 x H_{28}), 0.83 (br, 3H, 3 x H_{26a}), 0.79 (d, 3H, J = 5 Hz, 3 x H_{24a}), 0.67-0.74 (m, 1H, H_{18a}). ^{13}C NMR (125 MHz, $CDCl_3$, 25 °C): δ (ppm) 169.56, 168.69, 166.89, 165.48, 163.68, 163.56, 148.14, 140.51, 139.13, 138.83, 135.65, 134.54, 134.51, 133.49, 126.65, 129.64, 126.65, 129.64, 126.61, 124.78, 124.76, 123.53, 122.33, 118.13, 97.38, 82.84, 81.07, 78.50, 72.29, 70.24, 68.85, 68.16, 66.83, 61.39, 50.63, 41.49, 38.92, 36.81, 35.84, 35.49, 34.47, 33.34, 31.26, 29.08, 27.92, 27.43, 22.47, 21.40, 18.82, 17.45, 16.87, 14.60, 12.71, 11.72. HRMS: *m/z* $[M+Na]^+$for $C_{54}H_{68}N_6O_{14}$, calculated 1047.4685; observed 1047.4761. t_R (245 nm) = 14.25 min.

Ethyl 4-methyl-6-(4,5-dimethoxyphenyl)-2-((1-(2-oxo-2-(ivermectin aglycon-13-O-yloxy)ethyl)-1H-1,2,3-triazol-4-yl)methoxy)pyrimidine-5-carboxylate (19). Chromatographic eluent: Hexane/ethyl acetate (25:75, *v/v*). White solid. mp, 120 ºC. Yield: 81 %. IR: ν_{max} 3481.3, 2929.7, 1714.6, 1520.8, 1461.1, 1334.4, 1274.7, 1051.1, 991.5 cm^{-1}. ^{1}H NMR (500 MHz, $CDCl_3$, 25 °C): δ (ppm) 7.79 (s, 1H, triazole CH), 7.71 (s, 1H, ArH), 6.71 (s, 1H, ArH), 6.16-6.18 (m, 2H, H_9, -CHCOH), 5.64-5.79 (m, 4H, H_{10}, H_{11}, -OCH_2-), 5.22-5.33 (m, 4H, H_3, H_5, H_{13}, H_{19}),

4.96 (d, 1H, J = 10 Hz, H_{15}), 4.85 (s, 1H, -CHCOH, D_2O exchangeable), 4.50-4.59 (m, 2H, 2 x H_{8a}), 4.07–4.12 (m, 3H, -OCH_2CH_3, H_6), 4.00 (s, 3H, -OCH_3), 3.93 (s, 3H, -OCH_3), 3.70 (br, 1H, H_{17}), 3.59 (br, 1H, H_{25}), 3.21 (d, 1H, J = 5 Hz, H_2), 2.64-2.67 (m, 4H, H_{12}, -CH_3), 2.49-2.52 (m, 1H, H_{24}), 2.18-2.33 (m, 2H, 2 x H_{16}), 2.04 (s, 1H, C_5-OH, D_2O exchangeable), 1.87-1.95 (m, 2H, H_{18b}, H_{26}), 1.81 (d, 1H, J = 10 Hz, H_{20a}), 1.42-1.64 (m, 10H, 3 x H_{4a}, H_{20b}, 2 x H_{22}, 2 x H_{23}, 2 x H_{27}), 1.22 (d, 3H, J = 10 Hz, 3 x H_{14a}), 1.00-1.05 (m, 6H, 3H_{12a}, -OCH_2CH_3), 0.96 (t, 3H, 3 x H_{28}), 0.81 (d, 3H, J = 5 Hz, 3 x H_{24a}), 0.79 (br, 3H, 3 x H_{26a}), 0.67-0.72 (m, 1H, H_{18a}). ^{13}C NMR (125 MHz, $CDCl_3$, 25 °C): δ (ppm) 186.54, 170.57, 168.67, 166.00, 165.52, 163.40, 153.06, 149.03, 143.73, 140.47, 139.81, 138.80, 135.72, 133.50, 129.66, 126.57, 124.86, 122.33, 119.38, 118.10, 111.54, 107.24, 97.37, 82.83, 80.96, 78.49, 72.28, 68.83, 68.17, 66.82, 61.52, 61.41, 60.42, 56.68, 56.54, 50.56, 40.49, 38.93, 36.81, 35.84, 35.47, 34.48, 33.33, 31.26, 27.92, 27.43, 24.00, 21.08, 18.81, 17.44, 16.87, 14.60, 13.76, 12.70, 11.70. HRMS: *m/z* $[M+H]^+$ for $C_{55}H_{70}N_6O_{16}$, calculated 1071.4804; observed 1071.4794. t_R (245 nm) = 7.87 min.

Ethyl 4-methyl-6-phenyl-2-((1-(2-oxo-2-(ivermectin aglycon-13-O-yloxy)ethyl)-1H-1,2,3-triazol-4-yl)methoxy)pyrimidine-5-carboxylate (20). Chromatographic eluent: Hexane/ethyl acetate (35:65, *v/v*). White Solid. mp, 88 ºC. Yield: 77 %, IR: ν_{max} 3488.8, 2929.7, 1714.6, 1550.6, 1453.7, 1371.7, 1058.6, 991.5, 775.3 cm^{-1}. ^{1}H NMR (500 MHz, $CDCl_3$, 25 °C): δ (ppm) 7.85 (s, 1H, triazole CH), 7.64 (d, 1H, J = 5 Hz, ArH), 7.43-7.47 (m, 3H, ArH), 6.16-6.18 (m, 2H, H_9, -CHCOH), 5.63-5.79 (m, 4H, H_{10}, H_{11}, -OCH_2-), 5.23–5.33 (m, 4H, H_3, H_5, H_{13}, H_{19}), 4.96 (d, 1H, J = 10 Hz, H_{15}), 4.85 (s, 1H, -CHCOH, D_2O exchangeable), 4.50-4.59 (m, 2H, 2 x H_{8a}), 4.13-4.17 (q, 2H, -OCH_2CH_3), 4.06 (br, 1H, H_6), 3.68-3.70 (m, 1H, H_{17}), 3.58-3.60 (m, 1H, H_{25}), 3.21 (d, 1H, J = 5 Hz, H_2), 2.64-2.65 (m, 1H, H_{12}), 2.58 (s, 3H, -CH_3), 2.49-2.52 (m, 1H, H_{24}), 2.18-2.33 (m, 2H, 2 x H_{16}), 1.94 (d, 2H, J = 5 Hz, H_{18b}, H_{26}), 1.81 (d, 1H, J = 10 Hz, H_{20a}),

1.42-1.68 (m, 10H, 3 x H_{4a}, H_{20b}, 2 x H_{22}, 2 x H_{23}, 2 x H_{27}), 1.21 (d, 3H, J = 10 Hz, 3 x H_{14a}), 1.04 (m, 6H, 3 x H_{12a} ,-CH_3), 0.96 (t, 3H, 3 x H_{28}), 0.82 (d, 3H, J = 5 Hz, 3 x H_{24a}), 0.79 (br, 3H, J = 5 Hz, 3 x H_{26a}), 0.67-0.72 (m, 1H, H_{18a}). ^{13}C NMR (125 MHz, $CDCl_3$, 25 °C): δ (ppm) 168.94, 168.68, 168.19, 166.55, 165.48, 163.49, 144.17, 140.49, 138.82, 137.57, 135.67, 133.53, 130.23, 129.67, 128.45, 128.32, 126.59, 124.62, 122.37, 120.37, 118.09, 97.37, 82.85, 81.01, 78.50, 72.28, 68.84, 68.17, 66.82, 61.75, 61.27, 50.59, 40.49, 38.93, 36.81, 35.85, 35.48, 34.47, 33.34, 31.27, 29.68, 27.92, 27.42, 22.80, 18.81, 17.45, 16.88, 14.61, 13.61, 12.71, 11.72. HRMS: *m/z* $[M+H]^+$ for $C_{53}H_{67}N_5O_{12}$, calculated 966.4863; observed 966.5009. t_R(245 nm) = 12.11 min.

Synthesis of intermediates (21-23).

Intermediates of alkynes **10a** and **10c** were synthesized as reported,[38a] the synthesis of intermediates **21-23** of **10b** (Scheme 3) and characteristic data is presented below.

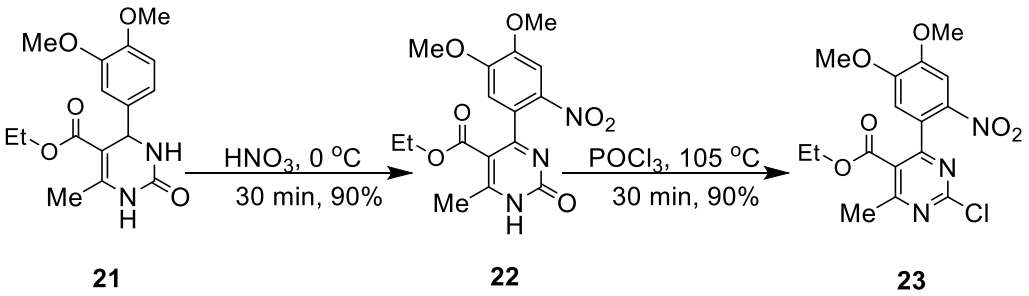

Scheme 3. Synthesis of intermediates of **10b.**

Synthesis of (22). To an ice cooled solution of conc. HNO_3 (10 ml), appropriate DHPM **21** (0.003 mol)[38b] was added over a period of 5 min. The resulting yellow solution was stirred for 30 min at 0 °C. Upon the completion of the reaction, the reaction mixture was poured into ice cooled water and neutralized with K_2CO_3. The resulting solution extracted with DCM (2×20 ml), dried over anhydrous sodium sulfate and solvent was evaporated to obtain yellow crude product,

which was purified by column chromatography over silica gel (60-120 mesh). Characteristic data is given below.

Ethyl 4-(4,5-dimethoxy-2-nitrophenyl)-6-methyl-2-oxo-1,2-dihydropyrimidine-5-carboxylate (22). Chromatographic eluent: ethyl acetate. Yellow solid. Yield: 92%. IR: ν_{max} 3108.6, 2981.9, 2840.2, 1699.7, 1647.5, 1580.4, 1513.3, 1326.9, 1267.7, 961.7, 872.2, 641.1 cm^{-1}. ^{1}H NMR (400 MHz, $CDCl_3$, 25 °C): δ (ppm) 7.73 (s, 1H, ArH), 6.75 (s, 1H, ArH), 4.00-4.06 (m, 2H, -$\underline{CH_2}CH_3$), 4.00 (s, 3H, -OCH_3), 3.96 (s, 3H,-OCH_3), 2.72 (s, 3H, -CH_3), 0.99 (t, 3H, 4Hz, -$CH_2\underline{CH_3}$).^{13}C NMR (100 MHz, $CDCl_3$, 25 °C): δ (ppm) 163.90, 157.96, 153.49, 149.14, 139.20, 110.77, 110.25, 106.96, 61.49, 56.74, 56.60, 29.76, 13.79. HRMS: *m/z* $[M+H]^+$ for $C_{16}H_{17}N_3O_7$, calculated 364.1139; observed 364.1351.

Synthesis of (23). Appropriate **22** (0.002 mol) was suspended in phosphorous oxychloride ($POCl_3$) (10 ml) and heated at 105 °C for 30 min. Excess ($POCl_3$) was removed under reduced pressure through azeotropic distillation with dry benzene to isolate a crude product, which was further purified by column chromatography over silica (60-120 mesh) using hexane/ethyl acetate as eluent. Characteristic data is given below.

Ethyl 2-chloro-4-(4,5-dimethoxy-2-nitrophenyl)-6-methylpyrimidine-5-carboxylate (23). Chromatographic eluent: hexane/ethyl acetate (90:10, v/v). Pale yellow solid. Yield: 91%. IR: ν_{max} 3063.9, 2944.6, 2847.7, 1729.5, 1520.8, 1334.4, 1274.7, 1222.6, 1051.1, 931.8, 767.3 cm^{-1}. ^{1}H NMR (400 MHz, $CDCl_3$, 25 °C): δ (ppm) 7.72 (s, 1H, ArH), 6.71 (s, 1H, ArH), 4.09 (q, 2H, 8Hz, -$\underline{CH_2}CH_3$), 3.94 (s, 3H, -OCH_3), 3.93 (s, 3H,-OCH_3), 2.68 (s, 3H, -CH_3), 1.02 (t, 3H, 8Hz, -$CH_2\underline{CH_3}$). ^{13}C NMR (100 MHz, $CDCl_3$, 25 °C): δ (ppm) 169.71, 166.50, 165.22, 160.62, 153.27,

149.61, 139.86, 126.63, 124.06, 111.64, 107.40, 62.24, 56.80, 56.70, 23.57, 13.81. HRMS: *m/z* $[M+H]^+$ for $C_{16}H_{16}ClN_3O_6$, calculated 382.0800; observed 382.1023.

Biology

***In vitro* activity against *P. berghei* hepatic stages**

In vitro activity of test compounds against the liver stage of *P. berghei* infection was assessed as previously described.[65,66] Briefly, Huh7 cells, a human hepatoma cell line, were routinely cultured in 1640 Roswell Park Memorial Institute (RPMI) medium supplemented with 10% (v/v) fetal bovine serum, 1% (v/v) glutamine, 1% (v/v) penicillin/streptomycin, 1% non-essential amino acids, and 10 mM HEPES. One day prior to infection, Huh7 cells were seeded at $1x10^4$ cell/well of a 96-well plate and incubated overnight at 37 ºC with 5% CO_2. 10 mM stock solutions of test compounds were prepared in DMSO and were serially diluted in infection medium, *i.e.* culture medium supplemented with gentamicin (50 µg/mL) and amphotericin B (0.8 µg/mL), in order to obtain the test concentrations. One hour prior to infection, culture medium was replaced by the serial dilutions of test compounds, followed by the addition of $1x10^4$ firefly luciferase-expressing *P. berghei* sporozoites, freshly isolated from the salivary glands of female infected *An. stephensi* mosquitoes. Plates were then centrifuged at 1800 xg for 5 min at room temperature and incubated at 37 ºC with 5% CO_2.

To assess the effect of each compound concentration in cell viability, infected cultures were incubated with Alamar Blue (Invitrogen, U.K.), according to the manufacturer's recommendations, at 46 h post infection (hpi). Parasite load was then assessed by a bioluminescence assay (Biotium, USA), using a multi-plate reader Infinite M200 (Tecan, Switzerland). The DMSO vehicle and the antiplasmodial drug atovaquone (ATQ) were used as negative and positive controls in these assays, respectively. Nonlinear regression analysis was

employed to fit the normalized results of the dose-response curves, and IC_{50} values were determined using GraphPad Prism 6.0 (GraphPad software, La Jolla, California, USA).

***In vitro* activity against *P. falciparum* blood stages**

Ring-stage synchronized cultures of *Pf*NF54 at 2.5% hematocrit and at approximately 1% parasitemia were incubated with drugs or DMSO (vehicle control) in 96 well-plates, for 48 h, at 37 °C in a 5% CO_2 and 5% O_2 atmosphere. Ten µM stock solutions of chloroquine, ivermectin and the compounds under evaluation were prepared in DMSO. Working solutions were prepared from the stock solutions in complete malaria culture medium (CMCM), which consists of RPMI 1640 supplemented with 25 mM HEPES, 2.4 mM L-glutamine, 50 µg/mL gentamicin, 0.5% w/v Albumax, 11 mM glucose, 1.47 mM hypoxanthine and 37.3 mM $NaHCO_3$. For each measurement, 5 µl of the culture (approximately 800 000 cells) were stained with the DNA-specific dye SYBR green I for 20 minutes, in the dark. Samples were then analyzed by flow cytometry (approximately 100,000 events per measurement). All samples were analyzed in triplicate and at least three different experiments were performed for each drug.

Insecticidal activity against *An. stephensi* mosquitoes

Balb/c mice (6-8 weeks old) were treated by a single oral administration of a 1 mg/kg suspension of compound **19**, compound **3** or ivermectin in sunflower oil. A suspension of an equivalent amount of DMSO in sunflower oil was used as control. Mosquitoes (~30 per mouse) were allowed to feed on treated or control mice for ~20 min in the dark 24 h after compound administration, and blood ingestion was confirmed by visual inspection. Mosquito survival was then assessed daily up to 14 days after ingestion of the blood meal. Two biological replicates were performed and mosquito survival results were pooled.

Ethics statement

All work with laboratory animals was performed according to National and European regulations (Directive 2010/63/EU). All protocols were approved by the animal experimentation ethics committee (AWB_2015_09_MP_Malaria) of the Instituto de Medicina Molecular-João Lobo Antunes and are in accordance with the Federation of European Laboratory Animal Science Associations (FELASA) guidelines.

ASSOCIATED CONTENT

Supporting Information

The Supporting Information is available free of charge on the ACS Publications website at DOI:

Additional data such as ^{1}H NMR spectra, ^{13}C NMR spectra, HRMS spectra, FTIR spectra and HPLC traces of compounds **1**,**3**,**16**,**17**,**19**,**20**. Assessment of *in vitro* activity of compounds/ivermectin derivatives against the hepatic stage of *P. berghei* infection and Mouse survival following spz administration and treatment using **19** and **3** (PDF). Molecular docking procedure for **19**. Molecular formula strings (CSV).

AUTHOR INFORMATION

Corresponding Author

*Kamaljit Singh: Department of Chemistry, Guru Nanak Dev University, Amritsar – 143 005, India. Tel: +91-183-2258802-09 (Extn. 3270), E-mail: kamaljit.chem@gndu.ac.in.

ORCID ID

Lovepreet Singh: 0000-0001-8256-1730

Diana Fontinha: 0000-0002-0046-648X

Denise Francisco: 0000-0003-1763-7107

António Mendes: 0000-0001-6562-5325

Miguel Prudêncio: 0000-0003-1746-6029

Kamaljit Singh: 0000-0002-9752-3363

Author Contributions

K.S. conceptualized the project and designed the hybrid compounds as well as the synthetic strategy. L.S. did synthesis, purification and characterization, and *in silico* docking studies under the supervision of K.S. M.P. designed and supervised all biological assays. D. Fontinha performed asexual blood stage assays, D. Francisco performed liver-stage assays and A.M.M. performed insecticidal assay. The manuscript was written through contributions of all authors. All authors have given approval to the final version of the manuscript.

Notes

The authors declare no competing financial interest.

ACKNOWLEDGMENTS

KS thanks SERB (DST) for the grant EMR/2017/000520 and Guru Nanak Dev University, Amritsar for funding under RUSA scheme as well as facilities. LS thanks University Grants Commission (UGC), New Delhi for Rajiv Gandhi National Fellowship. KS also thank Schrodinger (India) for providing complimentary access to Glide 2019. We are grateful to Ana Filipa Teixeira for the production and maintenance of *Anopheles stephensi* mosquitoes and for mosquito infections for sporozoite production. The biological study was supported by Fundação

para a Ciência e Tecnologia, Portugal (FCT-PT) Grant 02/SAICT/2017 (to MP). DF was supported by FEEI and FCT-MEC. AMM was supported by FCT-PT fellowship SFRH/BPD/80693/2011. MP was supported by FCT-PT Investigador FCT 2013 and CEEC 2018 fellowship.

ABBREVIATIONS

CQ^S, Chloroquine sensitive; CQ^R, Chloroquine resistant; GluCl, Glutamate-gated chloride channel; COSY, Correlation Spectroscopy, DMSO, Dimethyl sulfoxide, PDB, Protein Data Bank, TBDMS, *tert*-Butyldimethylsilyl, CMCM, Complete Malaria Culture Medium.

REFERENCES

1. World Health Organization (WHO). World Malaria Report 2019. http://www.who.int/malaria/publications/world-malaria-report-2019/report/en/ (accessed January 28, 2020).
2. World Health Organization (WHO). World Malaria Report 2018. http://www.who.int/malaria/publications/world-malaria-report-2018/report/en/ (accessed January 28, 2020).
3. Phillips, M. A.; Burrows, J. N.; Manyando, C.; Van Huijsduijnen, R. H.; Van Voorhis, W. C.; Wells, T. N. C. Malaria. *Nat. Rev. Dis. Prim.* **2017**, *3*, 17050.
4. Prudêncio, M.; Rodriguez, A.; Mota, M. M. The Silent Path to Thousands of Merozoites: the *Plasmodium* Liver Stage. *Nat. Rev. Microbiol.* **2016**, *4*, 849–856.
5. Cowman, A. F.; Healer, J.; Marapana, D.; Marsh, K. Malaria: Biology and Disease. *Cell* **2016**, *167*, 610–624.
6. White, N. J. Malaria Parasite Clearance. *Malar. J.* **2017**, *16*, 88.
7. Markus, M. B. Malaria: Origin of Term “Hypnozoite”. *J. Hist. Biol.* **2011**, *44*, 781-786.

8. Young, J. A.; Fivelman, Q. L.; Blair, P. L.; de la Vega, P.; Le Rochd, K. G.; Zhoud, Y.; Carucci, D. J.; Baker, D. A.; Winzeler, E. A. The *Plasmodium falciparum* Sexual Development Transcriptome: A Microarray Analysis Using Ontology-based Pattern Identification. *Mol. Biochem. Parasit.* **2005**, *143*, 67–79.

9. Yahia, S.; Rueda-Zubiaurre, A.; Delves, M. J.; Fuchter, M. J.; Baum, J. The Antimalarial Screening Landscape–Looking Beyond the Asexual Blood Stage. *Curr. Opin. Chem. Biol.* **2019**, *50*, 1–9.

10. Watson, J.; Taylor, W. R. J.; Bancone, G.; Chu, C. S.; Jittamala, P.; White, N. J. Implications of Current Therapeutic Restrictions for Primaquine and Tafenoquine in the Radical Cure of *Vivax* Malaria. *PLoS Negl. Trop. Dis.* **2018**, *12*, e0006440.

11. Baird, J. K.; Battle, K. E.; Howes, R. E. Primaquine Ineligibility in Anti-Relapse Therapy of *Plasmodium vivax* Malaria: The Problem of G6PD Deficiency and Cytochrome P-450 Polymorphisms. *Malar. J.* **2018**, *17*, 42.

12. Abilio, A. P.; Kleinschmidt, I.; Rehman, A. M.; Cuamba, N.; Ramdeen, V.; Mthembu, D. S.; Coetzer, S.; Maharaj, R.; Wilding, C. S.; Steven, A.; Coleman, M.; Hemingway, J.; Coleman, M. The Emergence of Insecticide Resistance in Central Mozambique and Potential Threat to the Successful Indoor Residual Spraying Malaria Control Programme. *Malar. J.* **2011**, *10*, 110.

13. White, N. J. Antimalarial Drug Resistance. *J. Clin. Invest*. **2004**, *113*, 1084–1092.

14. White, N. J. Antimalarial Drug Resistance and Combination Therapy. *Philos. Trans. R. Soc. Lond. B. Biol. Sci.* **1999**, *354*, 739–749.

15. Ogbonna, A.; Uneke, C. J. Artemisinin-Based Combination Therapy for Uncomplicated Malaria in Sub-Saharan Africa: The Efficacy, Safety, Resistance and Policy Implementation Since Abuja 2000. *Trans. R. Soc. Trop. Med. Hyg.* **2008**, *102*, 621–627.

16. Ajayi, N. A.; Ukwaja, K. N. Possible Artemisinin-Based Combination Therapy-Resistant Malaria in Nigeria: A Report of Three Cases. *Rev. Soc. Bras. Med. Trop.* **2013**, *46*, 525–527.

17. Sinden, R. E. Developing Transmission-Blocking Strategies for Malaria Control. *PLoS Pathog*. **2017**, *13*, e1006336.

18. Burg, R. W.; Miller, B. M.; Baker, E. E.; Birnbaum, J.; Currie, S. A.; Hartman, R.; Kong, Y. L.; Monaghan, R. L.; Olson, G.; Putter, I.; Tunac, J.B.; Wallick, H.; Stapley, E. O.; Oiwa, R.; Omura, S. Avermectins, New Family of Potent Anthelmintic Agents: Producing Organism and Fermentation. *Antimicrob. Agents Chemother*. **1979**, *15*, 361–367.

19. Omura, S. Ivermectin: 25 Years and Still Going Strong. *Int. J. Antimicrob. Agents.* **2008**, *31*, 91–98.

20. Crump, A.; Omura, S. Ivermectin, 'Wonder Drug' from Japan: Human Use Perspective. *Proc. Jpn. Acad. Ser. B Phys. Biol. Sci.* **2011**, *87*, 13–28.

21. Naquira, C.; Jimenez, G.; Guerra, J. G.; Bernal, R.; Nalin, D. R.; Neu, D.; Aziz, M. Ivermectin for Human *Strongyloidiasis* and Other Intestinal Helminths. *Am. J. Trop. Med. Hyg.* **1989**, *40*, 304–309.

22. Ohtaki, N.; Taniguchi, H.; Ohtomo, H. Oral Ivermectin Treatment in Two Cases of Scabies: Effective in Crusted Scabies Induced by Corticosteroids but Ineffective in Nail Scabies. *J. Dermatol*. **2003**, *30*, 411–416.

23. Curie, M. J.; Reynolds, G. J.; Glasgow, N. J.; Bowden, F. J. A Pilot Study of the Use of Oral Ivermectin to Treat Head Lice in Primary School Students in Australia. *Pedriatr. Dermatol.* **2010**, *27*, 595–599.

24. Nontasut, P.; Bussaratid, V.; Chullawichit, S.; Charoensook, N.; Visetsuk, K. Comparison of Ivermectin and Albendazole Treatment for Gnathostomiasis. *Southeast Asian J. Trop. Med. Public Health* **2000**, *31*, 374–379.

25. Shinohara, E. H.; Martini, M. Z., de Oliveira Neto, H. G.; Takahashi, A. Oral Myiasis Treated with Ivermectin: Case Report. *Braz. Dent. J.* **2004**, *15*, 79–81.

26. (a) Takiguchi, Y.; Mishima, H.; Okuda, M.; Terao, M.; Aoki, A.; Fakuda, R. Milbemycin, A New Family of Macrolide Antibiotics: Fermentation, Isolation and Physico-Chemical Properties. *J. Antibiot.* **1980**, *33*, 1120–1127. (b) Lo, L. C.; Berova, N.; Nakanishi, K.; Schlingmann, G.; Carter, G. T.; Borders, D. B. Determination of the Absolute Stereochemistry of Nemadectins $\propto_2$ and $\propto$. *J. Am. Chem. Soc.* **1992**, *114*, 7371-7374.

27. Slater, H. C.; Walker, P. G.; Bousema, T.; Okell, L. C.; Ghani, A. C. The Potential Impact of Adding Ivermectin to a Mass Treatment Intervention to Reduce Malaria Transmission: A Modelling Study. *J. Infect. Dis.* **2014**, *210*, 1972–1980.

28. Foy, B. D.; Kobylinski, K. C.; da Silva, I. M.; Rasgon, J. L.; Sylla, M. Endectocides for Malaria Control. *Trends Parasitol.* **2011**, *27*, 423–428.

29. Chaccour, C. J.; Kobylinski, K. C.; Bassat, Q.; Bousema, T.; Drakeley, C.; Pedro, A.; Foy, B. D. Ivermectin to Reduce Malaria Transmission: A Research Agenda for Promising New Tool for Elimination. *Malar. J.* **2013**, *12*, 153.

30. Kobylinski, K. C.; Foy, B. D.; Richardson, J. H. Ivermectin Inhibits the Sporogony of *Plasmodium falciparum* in *Anopheles gambiae*. *Malar. J.* **2012**, *11*, 381.

31. Chaccour, C.; Barrio, Á. I.; Gil Royo, A. G; Urbistondo, D. M.; Slater, H.; Hammann, F.; Del Pozo, J. L. Screening for an Ivermectin Slow-Release Formulation Suitable for Malaria Vector Control. *Malar. J.* **2015**, *14*, 102–110.

32. Panchal, M.; Rawat, K.; Kumar, G.; Kibria, K. M.; Singh, S.; Kalamuddin, M.; Mohmmed, A.; Malhotra, P.; Tuteja, R. *Plasmodium falciparum* Signal Recognition Particle Components and Anti-Parasitic Effect of Ivermectin in Nucleo-Cytoplasmic Shuttling of SRP. *Cell Death Dis*. **2014**, *5*, e994.

33. Mendes, A. M.; Albuquerque, I. S.; Machado, M.; Pissarra, J.; Míerless, P.; Prudêncio, M. Inhibition of *Plasmodium* Liver Infection by Ivermectin. *Antimicrob. Agents Chemother*. **2017**, *61*, 2e02005−16.

34. Singh, K.; Kaur, H.; Chibale, K.; Balzarini, J.; Little, S.; Bharatam, P. V. 2-Aminopyrimidine Based 4-Aminoquinoline Antiplasmodial Agents. Synthesis, Biological Activity, Structure Activity Relationship and Mode of Action Studies. *Eur. J. Med. Chem*. **2012**, *52*, 82–97.

35. Singh, K.; Kaur, H.; Chibale, K.; Balzarini, J. Synthesis of 4-Aminoquinoline-Pyrimidine Hybrids as Potent Antimalarials and their Mode of Action Studies. *Eur. J. Med. Chem.* **2013**, *66*, 314–323.

36. Singh, K.; Kaur, H.; Smith, P.; de Kock, C.; Chibale, K.; Balzarini, J. Quinoline-Pyrimidine Hybrids: Synthesis, Antiplasmodial Activity, SAR and Mode of Action Studies. *J. Med. Chem.* **2014**, *57*, 435–448.

37. Kaur, H.; Balzarini, J.; de Kock, C.; Smith, P.; Chibale, K.; Singh, K. Synthesis, Antiplasmodial Activity and Mechanistic Studies of Pyrimidine-5-Carbonitrile and Quinoline Hybrids. *Eur. J. Med. Chem.***2015**, *10*, 52–62.

38. Chopra, R.; de Kock, C.; Smith, P.; Chibale, K.; Singh, K. Ferrocene-Pyrimidine Conjugates: Synthesis, Electrochemistry, Physicochemical Properties and Antiplasmodial Activities. *Eur. J. Med. Chem.* **2015**, *100*, 1–9. (b) Singh, K.; Singh, J.; Deb, P. K.; Singh, H. An Expedient Protocol of The Biginelli Dihydropyrimidine Synthesis Using Carbonyl Equivalents. *Tetrahedron* **1999**, *55*, 12873-12880.

39. Chopra, R.; Chibale, K.; Singh, K. Pyrimidine-Chloroquine Hybrids: Synthesis and Antiplasmodial Activity. *Eur. J. Med. Chem.* **2018**, *148*, 39–53.

40. Kaur, H.; Machado, M.; de Kock, C.; Smith, P.; Chibale, K.; Prudêncio, M.; Singh, K. Primaquine-Pyrimidine Hybrids: Synthesis and Dual Stage Antiplasmodial Activity. *Eur. J. Med. Chem.* **2015**, *101*, 266–273.

41. Singh, K.; Kaur, T. Pyrimidine-Based antimalarials: Design Strategies and Antiplasmodial Effects. *Med. Chem. Commun.* **2016**, *7*, 749–768.

42. Gupta, P.; Singh, L.; Singh, K. The Hybrid Antimalarial Approach. *Medicinal Chemistry Approaches to Malaria and Other Tropical Diseases, In The Annual Reports In Medicinal Chemistry Series* (volume editor: Kelly Chibale), Elsevier (USA) (Chapter 3), **2019**, *53*, 73-105.

43. Meyers, J. I.; Gray, M.; Kuklinski, W.; Johnson, L. B; Snow, C. D.; Black, W. C., Partin, K. M.; Foy, B. D. Characterization of the Target of Ivermectin, the Glutamate-Gated Chloride Channel, from *Anopheles gambiae*. *J. Exp. Biol.* **2015**, *218*, 1478 –1486.

44. Hibbs, R. E.; Gouaux, E. Principles of Activation and Permeation in an Anion-Selective Cys-Loop Receptor. *Nature* **2011**, *474*, 54–60.

45. Zhao, J. H.; Xu, X. J.; Ji, M. J.; Cheng, J. L.; Zhu, G. N. Design, Synthesis, and Biological Activities of Milbemycin Analogues. *J. Agric. Food Chem.* **2011**, *59*, 4836–4850.

46. Shoop, W. L.; Mrozik, H.; Fisher, M. H. Structure and Activity of Avermectins and Milbemycin in Animal Health. *Vet. Parasitol*. **1995**, *59*, 139–156.

47. Rostovtsev, V. V.; Green, L. G.; Fokin, V. V.; Sharpless, K. B. A Stepwise Huisgen Cycloaddition Process: Copper (I) Catalyzed Regioselective "Ligation'' of Azides and Terminal Alkynes. *Angew. Chem. Int. Ed*. **2002**, *41*, 2596–2599.

48. Xu, Z.; Song, X. F.; Hu, Y. Q.; Qiang, M.; Lv, Z. S. Azide-Alkyne Cycloaddition Towards 1*H*-1,2,3 Triazole-Tethered Gatifloxacin and Isatin Conjugates: Design, Synthesis and *in vitro* Anti-Mycobacterial Evaluation. *Eur. J. Med. Chem.* **2017**, *138*, 66–71.

49. Duran. A.; Dogan, H. N.; Rollas, S. Synthesis and Preliminary Anticancer Activity of New 1,4-dihydro-3-(3-hydroxy-2-naphthyl)-4-substituted-5H-1,2,4-triazoline-5-thiones. *Farmaco*. **2002**, *57*, 559–564.

50. Gujjar, R.; Marwaha, A.; El Mazouni, F.; White, J.; White, L. K.; Creason, S.; Shackleford, D. M.; Baldwin. J.; Charman, W. N.; Buckner, F. S.; Charman, S.; Rathod, P. K.; Phillips, M. A. Identification of a Metabolically Stable Triazolopyrimidine-Based Dihydroorotate Dehydrogenase Inhibitor With Antimalarial Activity in Mice. *J. Med. Chem*. **2009**, *52*, 1864–1872.

51. Sztanke, K.; Tuzimski, T.; Rzymowska, J.; Pasternak, K.; Kendeferp-Szerszeń, M. Synthesis, Determination of the Lipophilicity, Anticancer and Antimicrobial Properties of Some Fused 1,2,4-Triazole Derivatives. *Eur. J. Med. Chem.* **2008**, *43*, 404–419.

52. Biot, C.; Glorian, G.; Maciejewski, L. A.; Brocard, J. S.; Domarle, O.; Blampain, G.; Millet, P.; Georges, A. J.; Abessolo, H.; Dive, D.; Lebibi, J. Synthesis and Antimalarial Activity *in Vitro* and *in Vivo* of a New Ferrocene-Chloroquine Analogue. *J. Med. Chem.* **1997**, *40*, 3715–3718.

53. Tripathi, M.; Taylor, D.; Khan, S. I.; Tekwani, B. L.; Ponnan, P.; Das, U. S.; Velpandian, T.; Rawat, D. S. Hybridization of Fluoro-Amodiaquine (FAQ) with Pyrimidines: Synthesis and Antimalarial Efficacy of FAQ-Pyrimidines. *ACS Med. Chem. Lett.* **2019**, *10*, 714–719.

54. Carrington, H. C.; Crowther, A. F.; Davey, D. G.; Levi, A. A.; Rose, F. L. A Metabolite of Paludrine with High Antimalarial Activity. *Nature* **1951**, *168*, 1080.

55. Falco, E. A.; Goodwin, L.G.; Hitchings, G. H.; Rollo, I. M.; Russel, P. B. 2: 4 Diaminopyrimidines- A New Series of Antimalarials. *Br. J. Pharmacol. Chemother*. **1951**, *6*, 185-200.

56. Jackson, H. C. Ivermectin as Systemic Insecticide. *Parasitol*. *Today* **1989**, *5*, 146–156.

57. Cully, D. F.; Vassilatis, D. K.; Liu, K. K.; Paress, P. S.; Van der Ploeg, L. H.; Schaeffer, J. M.; Arena, J. P. Cloning of an Avermectin-Sensitive Glutamate-Gated Chloride Channel from *Caenorhabditis elegans*. *Nature* **1994**, *371*, 707–711.

58. Kane, N. S.; Hirschberg, B.; Qian, S.; Hunt, D.; Thomas, B.; Brochu, R.; Ludmerer, S. W.; Zheng, Y.; Smith, M.; Arena, J. P.; Cohen, C. J.; Schmatz, D.; Warmke, J.; Cully, D. F. Drug resistant Drosophila Indicate Glutamate-Gated Chloride Channels are Targets for the Antiparasitics Nodulisporic Acid and Ivermectin. *Proc. Natl. Acad. Sci. USA*. **2000**, *97*, 13949–13954.

59. Cully, D. F.; Paress, P. S.; Liu, K. K.; Schaeffer, J. M.; Arena, J. P. Identification of a Drosophila Melanogaster Glutamate-Gated Chloride Channel Sensitive to the Antiparasitic Agent Avermectin. *J. Biol. Chem.* **1996**, *271*, 20187–20191.

60. Ludmerer, S. W.; Warren, V. A.; Williams, B. S.; Zheng, Y.; Hunt, D. C.; Ayer, M. B.; Wallace, M. A.; Chaudhary, A. G.; Egan, M. A.; Meinke, P. T.; Dean, D. C.; Garcia, M. L.; Cully, D. F.; Smith, M. M. Ivermectin and Nodulisporic Acid Receptors in Drosophila

Melanogaster Contain Both Gamma-Aminobutyric Acid-Gated Rdl and Glutamate-Gated GluCl Alpha Chloride Channel Subunits. *Biochemistry* **2002**, *41*, 6548-6560.

61. Dent, J. A.; Smith, M. M.; Vassilatis, D. K.; Avery, L. The Genetics of Ivermectin Resistance in *Caenorhabditis elegans*. *Proc. Natl. Acad. Sci. USA.* **2000**, *97*, 2674-2679.
62. Nasveld, P.; Russell, B.; Kotecka, B.; Rieckmann, K. Lack of *in Vitro* Effect of Ivermectin on *Plasmodium falciparum*. *Southeast Asian J. Trop. Med. Public Health* **2003**, *34*, 552–553.
63. Azevedo, R.; Mendes, A. M.; Prudêncio, M. Inhibition of *Plasmodium* Sporogonic Stages by Ivermectin and Other Avermectins. *Parasit. Vectors* **2019**, *12*, 549.
64. Kaur, S.; Dhoun, S.; Depotter, G.; Kaur, P.; Clays, K.; Singh, K. Synthesis, Linear and Nonlinear Optical Properties of Thermally Stable Ferrocene-Diketopyrrolopyrrole Dyads. *RSC Adv.* **2015**, *5*, 84643–84656.
65. Machado, M.; Sanches-Vaz, M.; Cruz, J. P.; Mendes, A. M.; Prudêncio, M. Inhibition of *Plasmodium* Hepatic Infection by Antiretroviral Compounds. *Front. Cell. Infect. Microbiol.* **2017**, *7*, 329.
66. Ploemen, I. H. J.; Prudêncio, M.; Douradinha, B. G.; Ramesar, J.; Fonager, J.; van Gemert, G.-J.; Luty, A. J. F.; Hermsen, C. C.; Sauerwein, R. W.; Baptista, F. G.; Mota, M. M.; Waters, A. P.; Que, I.; Lowik, C. W. G. M.; Khan, S. M.; Janse, C. J.; Franke-Fayard, B. M. D. Visualization and Quantitative Analysis of the Rodent Malaria Liver Stage by Real Time Imaging. *PLoS One* **2009**, *4*, e7881.

Table of Contents graphic

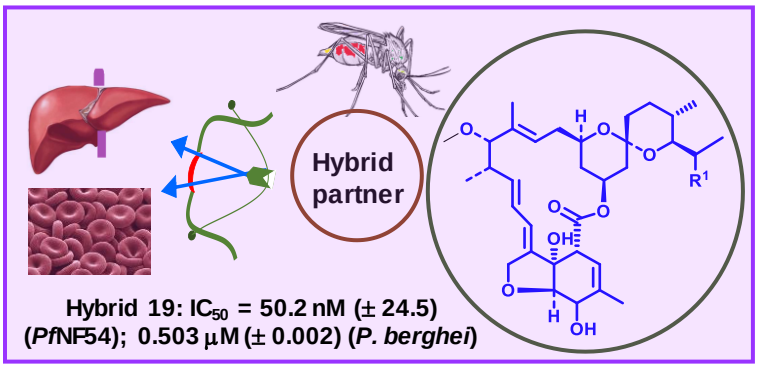

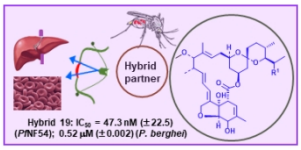

338x190mm (96 x 96 DPI)